

1 **MANUSCRIPT # 6884 REVISION 1**

2 **Carbonation and Decarbonation Reactions: Implications for Planetary Habitability**

3 E.M. STEWART^{1*}, JAY J. AGUE¹, JOHN M. FERRY², CRAIG M. SCHIFFRIES³, REN-BIAO
4 TAO⁴, TERRY.T. ISSON^{1,5}, AND NOAH J. PLANAVSKY¹

5 1: Yale University, Department of Geology & Geophysics, P.O. Box 208109, New Haven, CT
6 06520-8109, USA

7
8 2: Johns Hopkins University, Department of Earth and Planetary Sciences, 3400 N Charles
9 Street, Baltimore, MD 21218, USA

10 3: Carnegie Institution for Science, Geophysical Laboratory, 5251 Broad Branch Road NW,
11 Washington, DC 20015, USA

12 4: Peking University, School of Earth and Space Sciences, the MOE Key Laboratory of Orogenic
13 Belt and Crustal Evolution, Beijing 100871, CHINA

14 5: University of Waikato, Tauranga, NEW ZEALAND

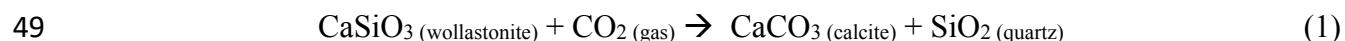
15
16 **correspondence: emily.stewart@yale.edu*

17 **ABSTRACT**

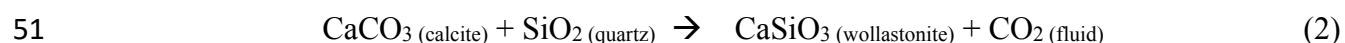
18 The geologic carbon cycle plays a fundamental role in controlling Earth's climate and
19 habitability. For billions of years, stabilizing feedbacks inherent in the cycle have maintained a
20 surface environment that could sustain life. Carbonation / decarbonation reactions are the
21 primary mechanism for transferring carbon between the solid Earth and the ocean-atmosphere
22 system. These processes can be broadly represented by the reaction: CaSiO_3 (wollastonite) + CO_2 (gas)
23 \Leftrightarrow CaCO_3 (calcite) + SiO_2 (quartz). This class of reactions is therefore critical to Earth's past and
24 future habitability. Here, we summarize their significance as part of the Deep Carbon
25 Observatory's 'Earth in Five Reactions' project. In the forward direction, carbonation reactions
26 like the one above describe silicate weathering and carbonate formation on Earth's surface.
27 Recent work aims to resolve the balance between silicate weathering in terrestrial and marine
28 settings both in the modern Earth system and through Earth's history. Rocks may also undergo
29 carbonation reactions at high temperatures in the ultramafic mantle wedge of a subduction zone
30 or during retrograde regional metamorphism. In the reverse direction, the reaction above
31 represents a variety of prograde metamorphic decarbonation processes which can occur in
32 continental collisions, rift zones, subduction zones, and in aureoles around magmatic systems.
33 We summarize the fluxes and uncertainties of major carbonation / decarbonation reactions and
34 review the key feedback mechanisms that are likely to have stabilized atmospheric CO_2 levels.
35 Future work on planetary habitability and Earth's past and future climate will rely on an
36 enhanced understanding of the long-term carbon cycle.

37 **INTRODUCTION**

38 Life has existed on planet Earth for more than three billion years. In that time there have
39 been profound changes in the brightness of the Sun, the temperature of the deep Earth, and even
40 the length of a day, yet throughout all of these changes the environment has remained stable
41 enough to support life. The global carbon cycle is generally agreed to have played a critical role
42 in maintaining this habitable climate on Earth. Carbon dioxide (CO₂) acts as a greenhouse gas, in
43 effect trapping solar energy and raising the temperature of the planet. Over geologic timescales
44 (about one million years or longer), carbon is exchanged between the solid Earth and the
45 atmosphere. The rate of atmospheric CO₂ removal increases with temperature, thus the exchange
46 acts as a global thermostat, stabilizing atmospheric CO₂ concentrations and therefore moderating
47 Earth's surface temperature. Carbon dioxide is exchanged between the solid Earth and the
48 atmosphere via carbonation reactions such as the archetypal:



50 and its reverse, decarbonation:



52 Consequently, these reactions are critical controls on the long-term atmospheric composition,
53 climate, and habitability of Earth, and they form an essential piece of the Deep Carbon
54 Observatory's 'Earth in Five Reactions' initiative (introduced by Li *et al.* 2019). Note that these
55 two simple reactions are used to represent many decarbonation/carbonation reactions involving
56 other cations (especially Mg²⁺) and other silicate minerals (see below).

57 Carbonation reactions such as reaction (1) occur when carbon in a gas or fluid reacts with
58 silicate minerals to form a solid, commonly a carbonate mineral. Studies of these reactions have

59 a long history in petrology and geochemistry. As early as 1894, the Swedish chemist Arvid G.
60 Högbom suggested that geologic processes could remove CO₂ from the atmosphere (Högbom
61 1894; see review by Berner 1995). In particular, the weathering of silicate rocks provides the
62 necessary chemistry to form carbonate minerals, ultimately transforming gaseous CO₂ into a
63 solid rock. This fundamental carbonation reaction was discussed in detail by Nobel Prize-
64 winning chemist Harold Urey more than 50 years later. In his 1952 book, *The Planets*, Urey
65 rearticulated the relationship between carbonate and silicate rocks, writing reaction (1), known
66 today as one of the “Urey Reactions.” Furthermore, he suggested that such reactions have
67 controlled atmospheric CO₂ concentrations throughout Earth history.

68 Decarbonation (e.g. reaction (2)) generally occurs when a rock containing carbonate
69 minerals, such as a siliceous limestone, is metamorphosed at elevated temperatures and
70 pressures. Victor Moritz Goldschmidt (1912) was the first to recognize the significance of
71 metamorphic decarbonation. Goldschmidt noted that the minerals quartz (SiO₂) and calcite
72 (CaCO₃) react to form wollastonite (CaSiO₃) and CO₂ gas when a rock is heated to a high
73 enough temperature; his was among the earliest to use thermodynamic principles to calculate a
74 mineral equilibrium and to quantitatively constrain the conditions of metamorphism.

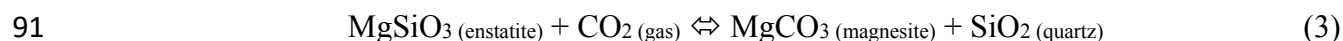
75 Norman L. Bowen (1940) demonstrated that, depending on bulk composition, 13
76 different decarbonation reactions may occur as a siliceous limestone or dolomite is progressively
77 heated. In 1956, Harker and Tuttle produced wollastonite in the laboratory via reaction (2).
78 Their experiments more tightly constrained the *P-T* (Pressure-Temperature) conditions of
79 reaction, yet, remarkably, Goldschmidt’s thermodynamic estimate from more than 40 years
80 earlier was quite close to their result.

81 Today, researchers continue to study carbonation / decarbonation reactions in essentially
82 all of Earth's geotectonic settings (Fig. 1) through numerical simulations, measurements of
83 modern CO₂ fluxes, and examination of the history preserved in the rock record. A detailed
84 accounting of the rates, timing, location, and magnitude of these reactions is essential to
85 understanding CO₂ fluxes and our planet's past, present, and future habitability.

86 CARBONATION

87 The Urey Reactions

88 The two Urey Reactions, one of which is mentioned above, are the quintessential
89 exemplars of carbonation reactions on Earth. The other reaction is quite similar to reaction (1)
90 and may run in parallel. The only difference is that it involves the Mg²⁺ cation instead of Ca²⁺:



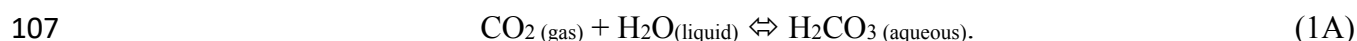
92 From here forward we will focus our discussion on reaction (1), but note that reaction (3)
93 functions essentially identically (Urey 1952).

94 In fact, reactions (1) and (3) as written do not often occur on the surface of the Earth. For
95 one, the mineral wollastonite actually makes up very little of the Earth's crust. About 50% of the
96 crust is composed of feldspars (e.g., Ronov *et al.* 1990). These are also silicate minerals, but with
97 more complicated chemistry and extensive solid solution. Plagioclase feldspars, for example, are
98 a solid solution between CaAl₂Si₂O₈ (anorthite) and NaAlSi₃O₈ (albite). In nature, weathering of
99 these more complex Ca-bearing silicates may produce phases in addition to calcite and quartz,
100 such as aluminous clays. Similarly, reaction (3) references the carbonate mineral magnesite,
101 which is also relatively rare on Earth's surface in its pure form. Thus reactions (1) and (3) are

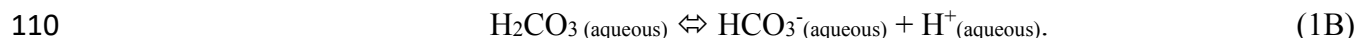
102 used as exemplars of carbonation reactions in general, but do not reflect the typical mineralogy
103 involved.

104 Additionally, on Earth's surface, carbonation reactions involve a series of reaction steps
105 as follows (after Siever 1968).

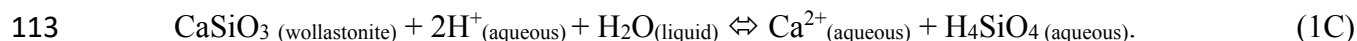
106 First, CO₂ gas in the atmosphere is dissolved in water (H₂O) to form carbonic acid (H₂CO₃):



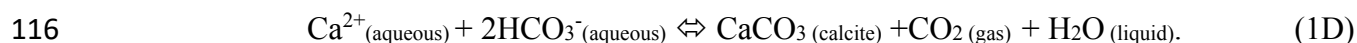
108 This carbonic acid can dissociate to form a negatively charged bicarbonate anion (HCO₃⁻) and
109 positively charged H⁺ cation:



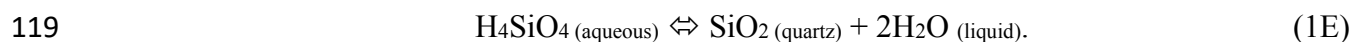
111 The acidity (H⁺ cations) in the water allows a calcium-bearing silicate mineral, here wollastonite
112 (CaSiO₃), to dissolve and form silicic acid (H₄SiO₄):



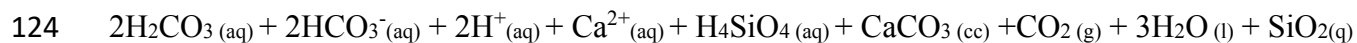
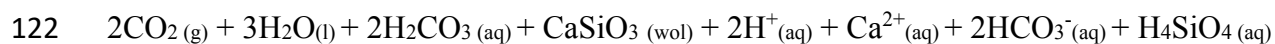
114 The Ca²⁺ cation is now free to react with the HCO₃⁻ anions to form the mineral calcite (CaCO₃),
115 more CO₂, and water:



117 Finally, the mineral quartz (SiO₂) may grow from the silicic acid in solution with more water as a
118 byproduct:



120 We can sum up these five sub-reactions (doubling reactions (1A) and (1B) for balance) to make
121 one total reaction:



125 and by cancelling species present on both sides of the reaction return to the simplified reaction
126 (1).

127 This reaction sequence has several important aspects to note. First, there are some
128 nuances of the full reaction (1F) that one cannot observe in the simplified reaction (1). For
129 example, the full reaction (1F) is only 50% efficient at storing CO₂; for every two molecules of
130 CO₂ which are dissolved in water, only one molecule is transformed into calcite while the other
131 molecule is re-released as CO₂ gas. Second, note also that each of the steps may occur at a
132 different point in space and time. A silicate mineral may weather and dissolve in a river in the
133 middle of a continent (reaction (1C)), but the Ca²⁺ ion may travel thousands of kilometers before
134 forming calcite in the ocean (reaction (1D)). Since the evolution of marine calcifiers, carbonate
135 mineral precipitation has often been facilitated by biological processes (e.g., the formation of a
136 foraminifera skeleton), although abiotic precipitation also occurs. In either case, formation of
137 carbonate minerals from solution functions as a key piece of this Urey reaction sequence.

138 The most important take-away from the Urey Reactions is this: surface carbonation
139 reactions are a major sink for atmospheric CO₂. In fact, more than 99% of all carbon in the crust,
140 biosphere, and ocean-atmosphere system is stored in sedimentary and metasedimentary rocks

141 (e.g., Archer 2010). Throughout Earth history, carbonation has been the primary way that CO₂ is
142 removed from the atmosphere (Urey 1952), and without this process life on Earth could not exist
143 (e.g., Berner & Caldeira 1997). For comparison, consider our neighboring planet, Venus, where
144 the Urey Reactions rarely occur. Much less carbon is stored in the solid rock of Venus, thus the
145 Venusian atmosphere contains massive amounts of CO₂, contributing to average surface
146 temperatures of more than 400 °C (Sagan 1962).

147 **Silicate Weathering**

148 On geologic timescales, silicate weathering is the rate-limiting step of the Urey reaction.
149 Because CO₂ dissolution, carbonic acid dissociation, and the other intermediate reactions occur
150 relatively quickly, the availability of silicate-bound Ca²⁺ (or Mg²⁺) (reaction (1C)) is of critical
151 importance. This can be thought of in terms of the seawater's alkalinity, that is, its ability to
152 neutralize acid. Silicate weathering increases the alkalinity of the seawater which drives
153 carbonate precipitation. Note that any contribution to total alkalinity drives carbonation, thus
154 weathering of Mg-silicate minerals could ultimately drive formation of Ca-carbonates.

155 Traditionally, geologists have considered continental rocks to be the primary contribution
156 to global silicate weathering (e.g., Walker *et al.* 1981; Berner *et al.* 1983). Continental
157 weathering depends on a sequence of discrete processes. First, continental rocks must be exposed
158 at Earth's surface. Surface rocks are then physically (or mechanically) eroded, that is, broken
159 apart into smaller pieces. Chemical weathering can then occur on the exposed surfaces (as seen
160 in Fig. 2A), partially dissolving the rock and releasing aqueous ions (i.e., reaction (1C)). There is
161 a positive association between physical erosion and chemical weathering – mineral dissolution
162 can contribute to denudation while erosion can expose more reactive surface area and facilitate

163 chemical weathering. The ions resulting from weathering are transported by rivers and ultimately
164 delivered to the ocean where they continue along the Urey Reaction sequence.

165 Many key factors can affect the rate of continental weathering. For example, tectonic
166 collisions which form high mountain belts help to expose more rock at Earth's surface, which
167 may increase the potential for weathering (e.g., Raymo & Ruddiman 1992; Edmond *et al.* 1995;
168 Dessert *et al.* 2003). Increased precipitation can lead to more physical erosion, and the additional
169 water can also drive more chemical weathering (H₂O is a necessary reactant in reaction 1C)
170 (Jenny 1941; Loughnan 1969; Amiotte *et al.* 1995; White & Blum 1995; Maher & Chamberlain
171 2014). At higher temperatures any chemical reaction will have a faster reaction rate (Arrhenius
172 1915); thus, increasing surface temperatures may result in faster continental weathering (Walker
173 1981; Berner *et al.* 1983; Manabe & Stouffer 1993).

174 **Marine Weathering**

175 More recently, some researchers have proposed that marine weathering processes have an
176 important role to play in global carbon cycling (e.g., Staudigel *et al.* 1989; Brady & Gisalson
177 1997; Wallmann *et al.* 2008; Coogan & Gillis 2013; Coogan & Dosso 2015). The concept is the
178 same – silicate minerals undergo chemical reaction which supplies alkalinity to the oceans and
179 helps form carbonate minerals. Marine weathering can occur within the marine sediment pile
180 (e.g., Wallmann *et al.* 2008; Solomon *et al.* 2014) or in basalts in 'off axis' hydrothermal
181 systems (Coogan & Dosso 2015). Evidence for chemical weathering of silicate minerals within
182 the sediment pile comes from deep anoxic (oxygen-free) sediments (Wallmann *et al.* 2008;
183 Solomon *et al.* 2014).

184 In ‘off-axis’ hydrothermal systems, large amounts of seawater flow through oceanic crust
185 (off-axis simply refers to the fact that these systems are not located directly adjacent to mid-
186 ocean ridge volcanoes). Along its flow path the water is heated to moderate temperatures (tens of
187 degrees C) and dissolves silicate minerals as in reaction (1C). Once again, this dissolution
188 delivers the alkalinity that allows carbonate minerals to form (e.g., Staudigel *et al.* 1989; Brady
189 & Gisalson 1997; Gillis & Coogan 2011). The impact these marine processes have on global
190 carbon cycling may be just as significant as the effect of continental weathering (e.g., Wallmann
191 *et al.* 2008; Coogan & Dosso 2015).

192 **Reverse Weathering**

193 Reverse weathering refers the formation of silicate clay minerals from solution. It is
194 ‘reverse’ weathering in the sense that it consumes the alkalinity and silica that the forward
195 silicate weathering reaction (1C) provides (Sillén 1961; Garrels 1965; Mackenzie & Garrels
196 1966). Reverse weathering is regarded as a net positive source of atmospheric CO₂. In other
197 words, reverse weathering allows for efficient recycling of carbon within the ocean-atmosphere
198 system, elevating atmospheric CO₂ concentrations. Recent work suggests that changes in the
199 amount of reverse weathering may have had profound climatic impacts over the course of Earth
200 history (Isson & Planavsky 2018).

201 **High – Temperature Carbonation in Subduction Zones and Orogens**

202 Carbonation reactions also take place deeper in Earth and at higher pressure-temperature
203 conditions. High-temperature carbonation occurs via many different reactions which are
204 exemplified by reaction (1). When CO₂-bearing fluid infiltrates a silicate rock (especially a mafic
205 or ultramafic rock with a high concentration of Mg²⁺) this fluid may react with the silicate

206 minerals, removing CO₂ from the fluid phase and forming new carbonate minerals (see Fig. 2B).
207 The particular silicate minerals involved in the reaction will depend upon the rock composition
208 and the *P-T* conditions.

209 One locus of such carbonation is the mantle wedge above a subducting slab (Falk &
210 Kelemen 2015, Piccoli *et al.* 2016, 2018; Scambelluri *et al.* 2016). As oceanic crust is subducted
211 into the mantle, it releases fluid into the overriding plate. This fluid may be dominantly H₂O, but
212 subduction zone decarbonation reactions may supply CO₂ as well (see section on decarbonation).
213 The ultramafic rocks of the mantle are highly reactive with CO₂ fluids, so when the slab-derived
214 fluid rises into the mantle, carbonation reactions are fast (Sieber *et al.* 2018). Because the degree
215 of carbonation increases with lower temperatures (Sieber *et al.* 2018), mantle wedge carbonation
216 probably dominates in the cooler (but still hot at < ~700 °C) fore-arc region and is less
217 pronounced in the hotter mantle directly below the volcanic arc.

218 The fate of this carbonated mantle is not well known. It may serve as a location of long-
219 term deep carbon storage (Kelemen & Manning 2015). Alternatively, melting of carbonated
220 mantle material may ultimately contribute CO₂ to the atmosphere when melt is erupted from
221 overlying arc volcanoes (Kerrick & Connolly 2001; Gorman *et al.* 2006; Kelemen & Manning
222 2015; Mason *et al.* 2017).

223 Similar high-temperature carbonation of ultramafic rocks can also occur in orogenic belts
224 during prograde regional (Evans & Trommsdorf 1974; Ferry *et al.* 2005) and contact (Ferry
225 1995) metamorphism. In addition, fluid infiltration during retrograde metamorphism (i.e.,
226 metamorphism as rocks cool down from peak *T*) may drive carbonation reactions. For example,
227 the mineral wollastonite is stable at high temperatures (Fig. 4). As the temperature falls, the

228 wollastonite will react with any available CO₂ to create calcite and quartz (Ferry 2000).
229 Critically, this retrograde carbonation reaction cannot occur in the absence of a CO₂-bearing
230 fluid (Tian and Ague 2014).

231 **DECARBONATION**

232 Decarbonation reactions, such as reaction (2), are a major source of atmospheric CO₂ in
233 geologic history. In the example reaction, a carbonate mineral (calcite) reacts with a silicate
234 mineral (quartz) to form the Ca-silicate mineral wollastonite and CO₂. Reaction (2) represents
235 myriad decarbonation reactions that all share these features: (1) a carbonate mineral reacts with a
236 silicate mineral, (2) a new silicate mineral is formed using divalent cations from the carbonate
237 (e.g. Ca²⁺, Mg²⁺, ...), and (3) CO₂ is released. (Rarely, decarbonation reactions may occur in the
238 absence of silicate minerals when a carbonate mineral breaks down into a mineral oxide and
239 CO₂).

240 Increasing temperature drives decarbonation. Certain carbonate-silicate mineral
241 assemblages (such as calcite and quartz) are only stable together up to a certain temperature at a
242 given pressure and fluid composition. When the temperature rises beyond that point they react
243 and release CO₂ (Goldschmidt 1912; Bowen 1940; Harker & Tuttle 1956). Figure 4 is a *P-T*
244 phase diagram, showing which mineral assemblage is stable at a given *P-T* condition and fluid
245 composition.

246 Therefore, these reactions generally occur when a mixed carbonate-silicate rock
247 undergoes significant increases in temperature and pressure (Goldschmidt 1912; Bowen 1940;
248 Harker & Tuttle 1956). On Earth, this can take place via prograde metamorphism, that is,

249 metamorphism of a rock driven in part by increasing temperature. Geologists recognize different
250 categories of metamorphism relating to different tectonic environments (Fig. 1).

251 **Contact Metamorphism**

252 Contact metamorphism occurs when a magma intrudes into solid rocks, and so can be
253 located anywhere volcanism and/or magmatism are active (Delesse 1858). In contact
254 metamorphism, rocks are not necessarily tectonically buried, they are simply heated by the
255 adjacent magma. Therefore, pure contact metamorphism is associated with higher geothermal
256 gradients (e.g., high temperatures at relatively low pressures) compared to regional
257 metamorphism. Additionally, it is more restricted in area, occurring in haloes (aureoles) around
258 magmatic intrusions. It has been suggested that degassing in contact aureoles around large
259 igneous provinces drove catastrophic global warming associated with some of Earth's largest
260 mass extinctions (e.g., Ganino & Arndt 2009; Burgess *et al.* 2017), but the relative importance of
261 this metamorphism remains debated (e.g., Nabelek *et al.* 2014).

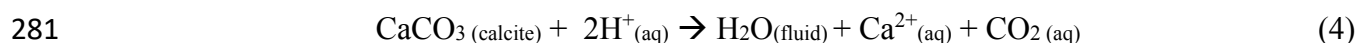
262 **Regional Metamorphism**

263 Regional-scale metamorphism takes place where two tectonic plates converge and
264 ultimately collide (subduction zones and continental collisions) or pull apart (e.g., continental
265 rifts) (Kennedy 1948; Miyashiro 1961). Figure 3 shows a map of both modern and ancient
266 collisional belts on Earth. As can be seen, such convergent plate boundaries are common
267 features. During regional-scale metamorphism rocks are subjected to both high pressures (~0.2 to
268 more than 2.0 GPa) and high temperatures (~250 up to ~1000 °C). Note that wollastonite is a
269 relatively uncommon mineral in regionally metamorphosed rocks, and other silicate minerals,
270 such as biotite and plagioclase, are more commonly produced (Ferry 1988).

271 **Decarbonation in Subduction Zones**

272 Subduction zones are a particularly important setting of CO₂ exchange. As oceanic crust
273 sinks into the mantle, it brings carbon-bearing minerals into the deeper Earth (Plank & Langmuir
274 1998). However, metamorphic decarbonation reactions in both the subducting slab and the
275 overriding plate may consume carbonate minerals and release CO₂ back toward the surface.
276 Thus, subduction may transfer carbon from the crust into the ocean-atmosphere system or into
277 the deep mantle.

278 Another mechanism of CO₂ production has recently been documented in subduction
279 zones. In the presence of a fluid, carbonate minerals may undergo congruent carbonate
280 dissolution such as:



282 (Frezzotti *et al.* 2011; Ague & Nicolescu 2014). The CO_{2(aq)} in reaction (4) represents aqueous
283 carbon species in general; carbonate and bicarbonate ions (Pann & Galli 2016) as well as organic
284 carbon species (Sverjensky *et al.* 2014) may be more important at depth. This reaction is
285 different from reaction (2) in two important ways: First, it does not require the presence of a
286 silicate mineral to proceed, and it could therefore occur in a pure carbonate rock. Second, it has
287 the potential to be highly efficient at releasing carbon. For example, in subducted rocks on the
288 Greek island of Syros carbonate dissolution released 60-90% of the solid carbon from the rock,
289 while decarbonation reactions might be expected to release less than ~3% (Ague & Nicolescu
290 2014). Thus, a small proportion of carbonate dissolution could have a relatively large effect.

291 Whatever the decarbonation mechanism, CO₂ released by subducting rocks may follow
292 several paths. It could flow through the many kilometers of overriding lithosphere (or perhaps
293 along the subduction interface) to escape to the atmosphere as part of a diffuse (i.e., spatially
294 widespread) metamorphic flux (e.g., Sakai *et al.* 1990; Sano & Williams 1996; Campbell *et al.*
295 2002), or it could become trapped in the overlying mantle wedge by a carbonation reaction (e.g.,
296 Piccoli *et al.* 2016, 2018; Scambelluri *et al.* 2016; Sieber *et al.* 2018). Once in the mantle wedge,
297 that carbon could be stored for millions of years. If carbonated mantle melts, however, this
298 carbon could form part of a magma and ultimately be released to the atmosphere as part of the
299 arc volcanic CO₂ flux (Varekamp 1992; Kelemen & Manning 2015; Poli 2015). Thus,
300 decarbonation in a subducted slab could contribute CO₂ to both a diffuse metamorphic flux and
301 the associated volcanic flux.

302 Decarbonation reactions also occur in the overriding plate in subduction zones, driven by
303 elevated temperatures from magma ascent and magmatic dewatering that would result in aqueous
304 fluid infiltration. This decarbonation flux should be more significant in continental arcs with
305 thick carbonate layers and less prominent when subduction occurs beneath oceanic crust (i.e.,
306 island arcs). Lee *et al.* (2013) recognized a relationship between total continental arc length and
307 global temperature in the past. They suggested that contact metamorphism-driven decarbonation
308 in these continental arcs may be an important source of atmospheric CO₂.

309 **Infiltration-driven Decarbonation**

310 The presence of a water-bearing fluid (either liquid or gas) has a profound effect on the
311 stability of carbonate minerals. Metamorphism in a closed system will not evolve much CO₂
312 until relatively high temperatures are reached (Greenwood 1975). On the other hand, infiltration

313 of a water-rich fluid into a reactive rock can depress the required temperature of a given
314 decarbonation reaction (e.g., Ferry 1976, 2016; Kerrick 1977; Penniston-Dorland & Ferry 2006;
315 Tracy *et al.* 1983; Ague 2002). This can be observed in zones of enhanced decarbonation around
316 fluid conduits as shown in Figure 2C. Classic studies in the metamorphic belts of the
317 Appalachian Mountains were among the first to demonstrate that fluid infiltration was essential
318 for driving reactions and releasing CO₂ (e.g. Ferry 1978, 1980; Rumble *et al.* 1982; Tracy *et al.*
319 *al.* 1983).

320 As a demonstration, we calculate the *P-T* conditions of reaction (2). When the X_{CO_2} (the
321 mole fraction of CO₂) in an H₂O – CO₂ fluid is low, the reaction can occur at a much lower
322 temperature. For example, at 0.2 GPa the reaction occurs at ~350 °C when $X_{CO_2} = 0.001$ and
323 ~700 °C when $X_{CO_2} = 1.0$ (Fig. 4).

324 This effect has two important implications. First, a rock that is metamorphosed in the
325 presence of a water-bearing fluid can release more than 500% more CO₂ than the metamorphism
326 of the same rock in a closed system at the same pressure and temperature (Stewart & Ague
327 2018). This enhanced decarbonation could ultimately result in a greater concentration of CO₂ in
328 the atmosphere and a correspondingly higher global surface temperature. Second, CO₂ generated
329 by infiltration is automatically released into a regional fluid flow system that provides the
330 mechanism for transporting evolved CO₂ from the deep crust to the atmosphere and hydrosphere.

331 **DISCUSSION: CARBON FLUXES AND PLANETARY HABITABILITY**

332 Carbonation / decarbonation reactions play a vital role in carbon transfer on Earth. In
333 order to understand how these reactions relate to planetary habitability, we must consider how
334 different processes interact and balance through the long-term (geologic) carbon cycle. A great

335 deal of the work done by geochemists focuses on constraining the magnitudes of major geologic
336 carbon fluxes. These fluxes are broadly divided into sources (inputs into the ocean–atmosphere
337 system) and sinks (outputs from the ocean–atmosphere system). Thus, decarbonation reactions
338 are sources of atmospheric CO₂ and carbonation reactions are sinks (Fig. 5).

339 **Carbonation Reaction Fluxes**

340 It is generally agreed that the primary long-term sink of CO₂ from the ocean-atmosphere
341 system is the precipitation of carbonate rocks using alkalinity derived from silicate weathering
342 (the Urey Reactions). The continental silicate weathering flux can be estimated from
343 measurements of river discharge, although on a very heterogeneous planet there are many
344 complexities to consider. Nevertheless, continental silicate weathering is estimated, with
345 reasonable uncertainty, to consume ~11.5 to 23 Tmol CO₂ yr⁻¹ (e.g., Gaillardet *et al.* 1999 and
346 references therein).

347 The marine silicate weathering flux is less studied. One estimate of CO₂ drawdown
348 resulting from chemical weathering of deep sea sediments is ~5 to ~20 Tmol CO₂ yr⁻¹,
349 comparable in magnitude to the continental flux (Wallmann *et al.* 2008). Off-axis carbonation of
350 basaltic oceanic crust may provide an additional sink of ~0.2 to ~3.7 Tmol CO₂ yr⁻¹ (e.g.,
351 Coogan & Gillis 2018 and references therein). However, reverse weathering recycles some CO₂
352 back into the surface environment, effectively acting as source of ~ 0.5 to ~1.25 Tmol CO₂ yr⁻¹
353 (Isson & Planavsky 2018).

354 **Decarbonation Reaction Fluxes**

355 Earth's major decarbonation reaction fluxes are the result of metamorphic outgassing
356 reactions in continental collisions, subduction zones, and contact metamorphic aureoles.
357 Metamorphism in continental rifts is less well-studied, but it may also make a significant
358 contribution.

359 Metamorphic outgassing in continental collisions has primarily been studied at the
360 regional scale. As shown by Stewart and Ague (2018), multiple estimates from ancient and
361 modern mountain belts converge on an area-normalized flux of $\sim 0.5 \times 10^6$ to $\sim 7 \times 10^6$ moles
362 $\text{CO}_2 \text{ km}^{-2} \text{ yr}^{-1}$ (Kerrick & Caldeira 1998; Chiodini *et al.* 2000; Becker *et al.* 2008; Skelton 2011).
363 These estimates are derived from independent, quite disparate methods, ranging from
364 thermodynamic modeling of metacarbonate rocks in the Appalachians (Stewart & Ague 2018) to
365 modern direct measurements of CO_2 escaping from springs in the Himalayas and Italian
366 Apennines (Chiodini *et al.* 2000; Becker *et al.* 2008). The agreement between estimates from
367 deeply exhumed rocks and measurements at Earth's surface suggests that most devolatilized CO_2
368 is ultimately released to the ocean-atmosphere system. We can multiply this areal flux estimate
369 by the area of active continental collision for a rough global collisional metamorphic flux. The
370 present area, dominated by the Himalayas with area $\sim 7.5 \times 10^5 \text{ km}^2$ (Becker *et al.* 2008), is
371 estimated on the order of $\sim 10^6 \text{ km}^2$. The resultant estimated global flux is ~ 0.5 to $\sim 7 \text{ Tmol CO}_2$
372 yr^{-1} , but note that this value is not constant through geologic time (Fig. 3).

373 Estimates of metamorphic degassing fluxes at subduction zones also cover a considerable
374 range. In their compilation, Kelemen & Manning (2015) estimate ~ 0.3 to $\sim 4.9 \text{ Tmol CO}_2 \text{ yr}^{-1}$ are
375 released from the slab via metamorphic reaction and dissolution. This estimate in itself carries
376 significant uncertainties, largely due to uncertainties in the degree and nature of fluid infiltration
377 during metamorphism. Closed-system calculations predict that the majority of subducted carbon

378 is not released (e.g., the negligible flux estimate from Kerrick & Connolly 2001). Models that
379 allow for fluid infiltration predict more decarbonation (e.g., 0.35 to 3.12 Tmol CO₂ yr⁻¹, Gorman
380 *et al.* 2006), with intermediate fluxes also suggested (Cook-Collars *et al.* 2014). Carbonate
381 dissolution, only recently identified in subduction zones (e.g., Ague & Nicolescu 2014), could
382 significantly increase these estimates.

383 In addition, it is highly uncertain what proportion of the devolatilized CO₂ makes it to the
384 atmosphere (either escaping through arc volcanoes or through its own diffuse outgassing) and
385 how much is stored in the overlying lithosphere. Kelemen & Manning (2015) report a diffuse
386 outgassing flux of ~0.3 to 1.0 Tmol CO₂ yr⁻¹, but emphasize that they suspect it might actually be
387 much larger.

388 Contact metamorphism, though spatially limited, has the potential to contribute large
389 quantities of CO₂. High temperature – low pressure conditions can drive decarbonation reactions
390 such as reaction (2) particularly efficiently. Contact metamorphism in particular may occur over
391 short timescales (e.g., Lyubetskaya & Ague 2010). The total contact metamorphic flux is
392 difficult to estimate, but some researchers suggest it has played an important role in changing
393 climate conditions through Earth history (e.g., Lee *et al.* 2013).

394 Although our discussion of CO₂ sources is focused on decarbonation reaction fluxes, we
395 can compare their magnitudes to other important CO₂ – generating fluxes. Typical estimates for
396 the three major volcanic fluxes in the modern era are as follows: ~1.5 to ~3.1 Tmol CO₂ yr⁻¹ for
397 arc volcanism (Marty & Tolstikhin 1998; Hilton *et al.* 2002; Dasgupta & Hirschmann 2010),
398 ~0.5 to ~5.0 Tmol CO₂ yr⁻¹ for mid-ocean ridge volcanism (Marty & Tolstikhin 1998; Dasgupta
399 & Hirschmann 2006, 2010; Le Voyer *et al.* 2019) and ~0.12 to ~3 Tmol CO₂ yr⁻¹ from ocean

400 island volcanoes (Marty & Tolstikhin 1998; Dasgupta & Hirschmann 2010). Volcanogenic CO₂
401 may also reach the atmosphere via diffuse outgassing (Allard 1992). Organic carbon weathering
402 is somewhat larger at ~7.5 to ~10 Tmol CO₂ yr⁻¹ (Holland 1978; Kump & Arthur 1999), but is
403 largely balanced out by the organic carbon burial flux of ~5.3 to ~ 10 Tmol CO₂ yr⁻¹ (Berner
404 1982; Kump & Arthur 1999). Thus, metamorphic outgassing fluxes are of the same order of
405 magnitude as other major source fluxes. Metamorphic decarbonation reactions are therefore
406 more important to the net global carbon budget than is often appreciated (Fig. 5).

407 **Earth's Habitability and the Need for Balance**

408 It has been commonly argued that surface temperatures on Earth have been remarkably
409 stable for billions of years. Sedimentary rocks record the presence of liquid water since at least
410 ~3.8 billion years ago (Lowe 1988) which requires global surface temperatures to remain
411 between 0 and 100 °C for a vast amount of time. Some researchers suggest there is evidence for
412 liquid water even earlier (e.g., 4.3 billion years ago by Mojzsis *et al.* 2001; 4.4 billion years ago
413 by Wilde *et al.* 2001).

414 In an apparent contradiction, the Sun has been increasing in luminosity and, therefore,
415 supplying more heat to Earth over time. It is estimated that the sun's luminosity in early Earth
416 history was only ~70% of the modern intensity (Sagan & Mullen 1972); thus, one might expect
417 Earth's temperature to have changed markedly in response to these changes in incoming solar
418 energy. As Sagan and Mullen pointed out in 1972, an Earth with today's atmospheric
419 composition would have been completely frozen (below 0 °C) until about 2 billion years ago.
420 This is at odds with geologic evidence for a warm climate early in Earth's history (e.g., Knauth
421 & Epstein 1976). This logical problem has been referred to as the 'Faint Young Sun Paradox',

422 and remains the subject of active debate today (see Kasting *et al.* 2010). However, one simple
423 solution to this paradox lies in Earth's atmosphere. A more carbon-rich atmosphere would result
424 in a more intense greenhouse effect and, perhaps, higher surface temperatures even with a
425 weaker sun (Owen *et al.* 1979; Walker *et al.* 1981).

426 On the other side of the spectrum, Earth has likewise never become too hot since the
427 emergence of the earliest life forms. If CO₂ concentrations became extremely high, the
428 temperature could skyrocket and the oceans could boil. Thus, we find ourselves on a type of
429 Goldilocks planet: CO₂ concentrations never get excessively high or excessively low, but, within
430 relatively narrow limits, they remain just right.

431 In their classic analysis, Berner & Caldeira (1997) argue that this cannot be a
432 coincidence. On long timescales, the amount of CO₂ added to the atmosphere must equal the
433 amount of CO₂ removed. Without this balance, atmospheric CO₂ concentrations would run-
434 away, resulting in extreme hot house or ice house climates. Berner & Caldeira (1997)
435 demonstrate this with a simple calculation of the effect of only small (25%) imbalances between
436 CO₂ inputs and outputs (Fig. 6).

437 Major CO₂ fluxes have been changing throughout Earth history. In order to maintain
438 balance, then, some stabilizing mechanism or negative feedback must be in place, ensuring that
439 inputs and outputs eventually reach a steady state. By simply summing modern flux estimates
440 (Fig. 5), we find that the predicted net change of the atmospheric reservoir is between ~ -45 and
441 ~ +11 Tmol CO₂ yr⁻¹. This estimate does overlap the necessary value of zero net change, but the
442 large uncertainty is obvious. Nonetheless, we can outline several different end-member Earth
443 states. With high weathering rate estimates (e.g., with large marine weathering fluxes; Wallman

444 *et al.* 2008, Coogan & Gillis 2018) upper-end member outgassing rates are required. High
445 amounts of reverse weathering (e.g., Rahman *et al.* 2017) could also help balance high silicate
446 weathering rates with outgassing estimates. In contrast, in the traditional view—where silicate
447 weathering occurs predominantly in continental settings—only the lowest outgassing fluxes
448 allow the modern Earth to be close to a steady state.

449 **The Continental Silicate Weathering Feedback.** The silicate weathering feedback is
450 the most prominent suggested mechanism for stabilizing the global carbon cycle. It was first
451 proposed by Walker *et al.* (1981) and states that the rate of continental silicate weathering and
452 resultant carbonate precipitation (whether abiotic or biologically mediated) speeds up at higher
453 temperatures and higher CO₂ concentrations. Recall that silicate weathering is the primary
454 pathway for removing CO₂ from the atmosphere, thus this constitutes a negative feedback: rising
455 CO₂ concentrations drive increasing global temperatures and increased silicate weathering
456 which, in turn, draws more CO₂ out of the atmosphere, lowering CO₂ concentrations and global
457 temperature.

458 This does not imply that CO₂ concentrations are essentially fixed throughout time. If CO₂
459 input fluxes are permanently doubled, the atmospheric CO₂ and temperature will not return to
460 previous values as a result of this feedback. Rather, the concentration of CO₂ and global
461 temperature will increase until the CO₂ output flux—silicate weathering—again matches the
462 inputs. The system will then reach a new steady state such that the concentration of CO₂ and the
463 temperature are higher than before, but they are stable. This also implies that there will be
464 periods of Earth history when inputs and outputs are *temporarily* imbalanced. For example,
465 Dutkiewicz *et al.* (2018) suggest that Cenozoic carbonation has outpaced solid earth

466 decarbonation, causing a global cooling trend. Recall, also, that the ‘faint young sun’ paradox of
467 Sagan & Mullen (1972) requires that the atmosphere has systematically lost CO₂ over billions of
468 years. As a consequence, feedback does not guarantee fixed temperatures, but it prevents run-
469 away warming or cooling trends.

470 The nature of the relationship between temperature and silicate weathering remains the
471 subject of vigorous debate. Some have proposed that global surface temperatures exert a direct
472 control on silicate weathering through a simple temperature-dependent reaction rate. In
473 laboratory experiments the rate of chemical weathering of silicate minerals (e.g., reaction (1C))
474 has been demonstrated to increase with increasing temperature (e.g., Lagache 1976; Brady &
475 Carroll 1994), yet in field studies results are mixed. Edmond *et al.* (1995) report no evidence of
476 increased chemical weathering at higher temperatures while Meybeck (1979) finds a significant
477 relationship. This work is complicated by the correlations between, for example, river runoff and
478 temperature that exist in nature.

479 Another possible mechanism relates CO₂ to chemical weathering directly: as atmospheric
480 CO₂ concentrations increase, more CO₂ will be dissolved in water to form carbonic acid. This
481 more acidic surface environment could also contribute to faster chemical weathering of silicate
482 minerals (e.g., Berg & Banwart 2000). This factor is likely more important prior to the rise of
483 land plants and the onset of extensive soil respiration.

484 Most research today focuses on indirect relationships between temperature and silicate
485 weathering. In particular, higher temperatures drive increased global precipitation rates and
486 increased river runoff (Holland 1978; Manabe & Stouffer 1993). Therefore, many models
487 suggest that it is primarily this invigoration of the water cycle which enhances silicate

488 weathering and CO₂ drawdown (Berner & Berner 1997; Maher & Chamberlain 2014). Teasing
489 out the influence of temperature, precipitation, or other factors can be extremely challenging in
490 such complex systems, but modern statistical techniques (e.g., machine learning) could be an
491 effective means to probe the factors driving the silicate weathering feedback.

492 **Marine Weathering Feedback.** Because weathering of continental material has
493 historically been considered as the primary contribution to global silicate weathering, it has also
494 been assumed to be the source of the associated negative feedback. However, recent studies
495 have demonstrated that seafloor weathering and carbonation may offer an additional,
496 complementary negative feedback. The general idea is the same: rising CO₂ concentrations and
497 global temperatures increase the rate of marine weathering, thereby drawing down more CO₂ and
498 stabilizing the system. Indeed, off-axis hydrothermal alteration of basaltic crust is enhanced at
499 higher temperatures (Coogan & Dosso 2015). The rate of silicate mineral dissolution will be
500 significantly faster when the ocean bottom water temperature is elevated. On the other hand, it
501 has been suggested that chemical weathering of marine anoxic sediments is largely independent
502 of temperature (Wallmann *et al.* 2008). Importantly, CO₂ that is stored in oceanic crust may in
503 the future contribute to a metamorphic decarbonation flux when it is inevitably subducted (Fig.
504 1).

505 **Reverse Weathering Feedback.** It was recently proposed that reverse weathering can act
506 as an important stabilizing feedback for carbon cycling (Isson & Planavsky 2018). In this case,
507 increasing atmospheric CO₂ makes the ocean more acidic, reducing the amount of clay
508 formation, and thus CO₂ release, from reverse weathering. This, in turn, lowers atmospheric
509 CO₂, pushing ocean water pH back towards less acidic values. Today this feedback is less
510 effective – clay formation is limited by the availability of SiO₂ dissolved in the ocean. There is

511 evidence, however, that this process was much more important early in Earth's history. Prior to
512 the Cambrian Period (~542 million years ago) oceanic silica concentrations were much higher.
513 This would allow for more reverse weathering and, perhaps, enhanced efficiency of a reverse
514 weathering negative feedback (Isson & Planavsky 2018).

515 **IMPLICATIONS**

516 **Future Work**

517 Major gaps remain in our understanding of global carbonation / decarbonation reactions.
518 More work is needed on constraining the magnitude of the various carbon fluxes and how they
519 balance one another throughout time. One area of particular uncertainty is the fate of subducted
520 carbon. As of today, it is unknown whether most of the carbonate minerals in the oceanic crust
521 are ultimately delivered to the deep mantle, or if they devolatilize during subduction. And for the
522 CO₂ that does escape the down-going slab, is most of it ultimately released to the atmosphere, or
523 is it stored in the subarc lithosphere (Kelemen & Manning 2015)? Observations made in ancient
524 and modern subduction zones in concert with constraints from experiments and numerical
525 modeling must begin to answer these questions if we are to make progress in a global
526 understanding of carbon mobility.

527 Another significant uncertainty is the strength of the silicate weathering feedback. This
528 feedback is not perfectly efficient – the Earth has swung between hot house and ice house
529 conditions many times in the past (e.g., Royer *et al.* 2004). In fact, the strength of the feedback is
530 certainly not fixed. We see evidence for periods of reduced and enhanced feedback efficiency in
531 the geologic record (e.g., Caves *et al.* 2016). Nevertheless, the ability to constrain the magnitude
532 of the effect of silicate weathering in ancient and modern Earth systems will allow us to make

533 more accurate calculations of past and future climate. Both theoretical (e.g., Winnick & Maher
534 2018) and observational approaches could provide valuable new insights.

535 There is limited work on the behavior of carbonate minerals at high pressures. For
536 example, recent work suggests carbon in subduction zones is hosted in the minerals dolomite and
537 magnesite (Tao *et al.* 2018), yet experimental constraints on their solubilities at these conditions
538 are lacking. Recent theoretical work is addressing the issue (e.g., Sverjensky *et al.* 2014;
539 Connolly & Galvez 2018), but should be supplemented by a new generation of experimental
540 data.

541 **Exoplanet Habitability**

542 Each of the processes discussed has important implications in the study of distant
543 exoplanets and our search for other habitable worlds. The presence of a silicate weathering
544 feedback, for example, will significantly increase the size of the “habitable zone” around a given
545 star—the range of planetary distances from the star that fall within a habitable temperature range
546 (Kasting *et al.* 1993). The balance between continental and marine weathering feedbacks is also
547 important. If marine weathering is *not* a significant negative feedback mechanism, then we
548 would not expect planets that are mostly ocean (“water worlds”) to have a stable, habitable
549 climate (Abbot *et al.* 2018). If on the other hand, marine weathering is strongly temperature
550 dependent, these worlds would be more likely to sustain life. The presence of volcanism and/or
551 plate tectonics could also have profound effects on an exoplanet’s carbon cycle and potential
552 habitability (e.g., Sleep & Zahnle 2001). Studying these processes on Earth may lead to better
553 predictions of which distant planets might be hospitable to life.

554 **Carbonation Reactions and Anthropogenic Climate Change**

555 Since the industrial revolution, Earth's global carbon cycle has been subject to a fast and
556 massive perturbation, evidently unequaled in geologic history. Through burning of fossil fuels,
557 deforestation, and other human activity, ~795 Tmol CO₂ are added to the ocean-atmosphere
558 system every year (Friedlingstein *et al.* 2010). This is more than one hundred times greater than
559 the global volcanic CO₂ flux or, as Gerlach (2011) notes, equivalent to about 9500 Kilauea
560 volcanoes. One could, perhaps, take comfort in the knowledge that the natural geologic carbon
561 cycle can eventually stabilize global temperatures, but most will consider a lag time of about 1
562 million years unacceptable. With this in mind, some researchers are attempting to harness and
563 accelerate the power of silicate weathering to counteract human-driven climate change in our
564 lifetimes (O'Connor *et al.* 2000; Lackner 2003; Park & Fan 2004; Kelemen & Matter 2008; Lal
565 2008; Wilson *et al.* 2009; Lechat *et al.* 2016; Power *et al.* 2016; Kelemen *et al.* 2018).

566 In many cases ultramafic rocks are used. These rocks are composed of Mg-rich minerals
567 that are particularly unstable at Earth's surface, which facilitates dissolution (like reaction (1C))
568 and subsequent carbonation. In some cases, these rocks are merely ground up and exposed at
569 Earth's surface to undergo natural reaction with the atmosphere (e.g., Lechat *et al.* 2016), while
570 other studies consider more active processes, such as pumping a CO₂ rich fluid through the rocks
571 (this is more similar to off-axis hydrothermal alteration; e.g., Park & Fan 2004; Matter *et al.*
572 2016). In either case, understanding natural geologic carbonation reactions has the potential to
573 inform future work on carbon sequestration and contribute to the continued habitability of planet
574 Earth.

575

ACKNOWLEDGEMENTS

576 We would like to thank the Deep Carbon Observatory and specifically the Reservoirs and Fluxes
577 Community and the attendees of the 2018 ‘The Earth in Five Reactions’ workshop for their
578 support of this work. We are grateful for helpful discussions with G.E. Bebout, R.A. Berner, O.
579 Beyssac, A.V. Brovarone, C.P. Chamberlain, D.A.D. Evans, M.E. Galvez, B. Marty, F. Piccoli,
580 D. Rumble, D.M. Rye, M. Tian, and J.L.M. van Haren. This work also benefits from constructive
581 reviews by A.D.L. Skelton and an anonymous reviewer. Funding provided by the National
582 Science Foundation (EAR–1650329 to JJA) and Yale University is gratefully acknowledged.

583 REFERENCES CITED

- 584
585 Abbot, D. S., Cowan, N. B., & Ciesla, F. J. (2012). Indication of insensitivity of planetary
586 weathering behavior and habitable zone to surface land fraction. *The Astrophysical*
587 *Journal*, 756(2), 178.
588
589 Ague, J. J. (2002). Gradients in fluid composition across metacarbonate layers of the Wepawaug
590 Schist, Connecticut, USA. *Contributions to Mineralogy and Petrology*, 143(1), 38-55.
591
592 Ague, J. J. (2003). Fluid infiltration and transport of major, minor, and trace elements during
593 regional metamorphism of carbonate rocks, Wepawaug Schist, Connecticut,
594 USA. *American Journal of Science*, 303(9), 753-816.
595
596 Ague, J. J., & Nicolescu, S. (2014). Carbon dioxide released from subduction zones by fluid-
597 mediated reactions. *Nature Geoscience*, 7(5), 355.
598
599 Allard, P. (1992). Diffuse degassing of Carbon Dioxide through volcanic systems: observed facts
600 and implications. *Report Geol. Sur. of Japan*, 7-11.
601
602 Amiotte Suchet, P., and Probst, J. L. (1995). A global model for present-day atmospheric: Soil
603 CO₂ consumption by chemical erosion of continental rocks (GEM-CO₂): *Tellus*, v. 47B,
604 p. 273–280.
605
606 Archer, D. (2010), *The Global Carbon Cycle*, 205 pp., Princeton Univ. Press, Princeton, N. J.
607
608 Arrhenius, S. (1915). *Quantitative laws in biological chemistry* (Vol. 1915). G. Bell.
609
610 Becker, J. A., Bickle, M. J., Galy, A., & Holland, T. J. (2008). Himalayan metamorphic CO₂
611 fluxes: Quantitative constraints from hydrothermal springs. *Earth and Planetary Science*
612 *Letters*, 265(3-4), 616-629.
613
614 Berg, A., & Banwart, S. A. (2000). Carbon dioxide mediated dissolution of Ca-feldspar:

- 615 implications for silicate weathering. *Chemical Geology*, 163(1-4), 25-42.
616
- 617 Berner, R. A. (1982). Burial of organic carbon and pyrite sulfur in the modern ocean: its
618 geochemical and environmental significance. *American Journal of Science*, 282, 451-
619 473.
620
- 621 Berner, R. A. (1995). AG Högbom and the development of the concept of the geochemical
622 carbon cycle. *American journal of science*, 295(5), 491-495.
623
- 624 Berner, R. A., & Berner, E. K. (1997). Silicate weathering and climate. In *Tectonic uplift and*
625 *climate change* (pp. 353-365). Springer, Boston, MA.
626
- 627 Berner, R. A., & Caldeira, K. (1997). The need for mass balance and feedback in the
628 geochemical carbon cycle. *Geology*, 25(10), 955-956.
629
- 630 Berner, R. A., Lasaga, A. C., and Garrels, R. M. (1983). The carbonate-silicate geochemical
631 cycle and its effect on atmospheric carbon dioxide over the past 100 million years:
632 *American Journal of Science*, 283, 641-683.
633
- 634 Bowen, N. L. (1940). Progressive metamorphism of siliceous limestone and dolomite. *The*
635 *Journal of Geology*, 48(3), 225-274.
636
- 637 Brady, P. V., & Carroll, S. A. (1994). Direct effects of CO₂ and temperature on silicate
638 weathering: Possible implications for climate control. *Geochimica et Cosmochimica*
639 *Acta*, 58(7), 1853-1856.
640
- 641 Brady, P. V., & Gislason, S. R. (1997). Seafloor weathering controls on atmospheric CO₂ and
642 global climate. *Geochimica et Cosmochimica Acta*, 61(5), 965-973.
643
- 644 Burgess, S. D., Muirhead, J. D., & Bowring, S. A. (2017). Initial pulse of Siberian Traps sills as
645 the trigger of the end-Permian mass extinction. *Nature communications*, 8(1), 164.
646
- 647 Burke, K., Dewey, J. F., & Kidd, W. S. F. (1977). World distribution of sutures—the sites of
648 former oceans. *Tectonophysics*, 40(1-2), 69-99.
649
- 650 Caves, J. K., Jost, A. B., Lau, K. V., & Maher, K. (2016). Cenozoic carbon cycle imbalances and
651 a variable weathering feedback. *Earth and Planetary Science Letters*, 450, 152-163.
652
- 653 Campbell, K. A., Farmer, J. D., & Des Marais, D. (2002). Ancient hydrocarbon seeps from the
654 Mesozoic convergent margin of California: carbonate geochemistry, fluids and
655 palaeoenvironments. *Geofluids*, 2(2), 63-94.
656
- 657 Chiodini, G., Frondini, F., Cardellini, C., Parello, F., & Peruzzi, L. (2000). Rate of diffuse carbon
658 dioxide Earth degassing estimated from carbon balance of regional aquifers: the case of
659 central Apennine, Italy. *Journal of Geophysical Research: Solid Earth*, 105(B4), 8423-
660 8434.

- 661
662 Connolly, J. A., & Galvez, M. E. (2018). Electrolytic fluid speciation by Gibbs energy
663 minimization and implications for subduction zone mass transfer. *Earth and Planetary*
664 *Science Letters*, 501, 90-102.
665
666 Coogan, L. A., & Dosso, S. E. (2015). Alteration of ocean crust provides a strong temperature
667 dependent feedback on the geological carbon cycle and is a primary driver of the Sr-
668 isotopic composition of seawater. *Earth and Planetary Science Letters*, 415, 38-46.
669
670 Coogan, L. A., & Gillis, K. M. (2013). Evidence that low-temperature oceanic hydrothermal
671 systems play an important role in the silicate-carbonate weathering cycle and long-term
672 climate regulation. *Geochemistry, Geophysics, Geosystems*, 14(6), 1771-1786.
673
674 Coogan, L. A., & Gillis, K. M. (2018). Low-Temperature Alteration of the Seafloor: Impacts on
675 Ocean Chemistry. *Annual Review of Earth and Planetary Sciences*, 46, 21-45.
676
677 Cook-Kollars, J., Bebout, G. E., Collins, N. C., Angiboust, S., & Agard, P. (2014). Subduction
678 zone metamorphic pathway for deep carbon cycling: I. Evidence from HP/UHP
679 metasedimentary rocks, Italian Alps. *Chemical Geology*, 386, 31-48.
680
681 Dasgupta, R., & Hirschmann, M. M. (2006). Melting in the Earth's deep upper mantle caused by
682 carbon dioxide. *Nature*, 440(7084), 659.
683
684 Dasgupta, R., & Hirschmann, M. M. (2010). The deep carbon cycle and melting in Earth's
685 interior. *Earth and Planetary Science Letters*, 298(1-2), 1-13.
686
687 de Capitani, C., & Petrakakis, K. (2010). The computation of equilibrium assemblage diagrams
688 with Theriak/Domino software. *American Mineralogist*, 95(7), 1006-1016.
689
690 Delesse, A. (1858). *Etudes sur la métamorphisme des roches*. Annales de Mines. E. Thunot:
691 Paris.
692
693 Dessert, C., Dupré, B., Gaillardet, J., François, L. M., & Allegre, C. J. (2003). Basalt weathering
694 laws and the impact of basalt weathering on the global carbon cycle. *Chemical Geology*,
695 202(3-4), 257-273.
696
697 Dutkiewicz, A., Müller, R. D., Cannon, J., Vaughan, S., & Zahirovic, S. (2018). Sequestration
698 and subduction of deep-sea carbonate in the global ocean since the Early Cretaceous.
699 *Geology*, 47(1), 91-94.
700
701 Edmond, J. M., Palmer, M. R., Measures, C. I., Grant, B., & Stallard, R. F. (1995). The fluvial
702 geochemistry and denudation rate of the Guayana Shield in Venezuela, Colombia, and
703 Brazil. *Geochimica et Cosmochimica Acta*, 59(16), 3301-3325.
704
705 Evans, B. W., & Trommsdorff, V. (1974). Stability of enstatite + talc and CO₂-metasomatism of

- 706 metaperidotite, Val d'Efra, Lepontine Alps. American Journal of Science, 274(3), 274-
707 296.
708
- 709 Falk, E. S., & Kelemen, P. B. (2015). Geochemistry and petrology of listvenite in the Samail
710 ophiolite, Sultanate of Oman: complete carbonation of peridotite during ophiolite
711 emplacement. *Geochimica et Cosmochimica Acta*, 160, 70-90.
712
- 713 Ferry, J. M. (1976). Metamorphism of calcareous sediments in the Waterville-Vassalboro area,
714 South-central Maine; mineral reactions and graphical analysis. *American Journal of*
715 *Science*, 276(7), 841-882.
716
- 717 Ferry, J. M. (1978). Fluid interaction between granite and sediment during metamorphism,
718 south-central Maine. *American Journal of Science*, 278(8), 1025-1056.
719
- 720 Ferry, J. M. (1980). A case study of the amount and distribution of heat and fluid during
721 metamorphism. *Contributions to Mineralogy and Petrology*, 71(4), 373-385.
722
- 723 Ferry, J. M. (1988). Infiltration-driven metamorphism in northern New England, USA. *Journal of*
724 *Petrology*, 29(6), 1121-1159.
725
- 726 Ferry, J. M. (1995). Fluid flow during contact metamorphism of ophicarbonates in the
727 Bergell aureole, Val Malenco, Italian Alps. *Journal of Petrology*, 36(4), 1039-1053.
728
- 729 Ferry, J. M. (2000). Patterns of mineral occurrence in metamorphic rocks. *American*
730 *Mineralogist*, 85(11-12), 1573-1588.
731
- 732 Ferry, J. M. (2016). Fluids in the crust during regional metamorphism: Forty years in the
733 Waterville limestone. *American Mineralogist*, 101(3), 500-517.
734
- 735 Ferry, J. M., Rumble, D., Wing, B. A., & Penniston-Dorland, S. C. (2005). A New Interpretation
736 of Centimetre-scale Variations in the Progress of Infiltration-driven Metamorphic
737 Reactions: Case Study of Carbonated Metaperidotite, Val d'Efra, Central Alps,
738 Switzerland. *Journal of Petrology*, 46(8), 1725-1746.
739
- 740 Friedlingstein, P., Houghton, R. A., Marland, G., Hackler, J., Boden, T. A., Conway, T. J., ... &
741 Le Quere, C. (2010). Update on CO₂ emissions. *Nature geoscience*, 3(12), 811.
742
- 743 Gaillardet, J., Dupré, B., Louvat, P., & Allegre, C. J. (1999). Global silicate weathering and CO₂
744 consumption rates deduced from the chemistry of large rivers. *Chemical geology*, 159(1-
745 4), 3-30.
746
- 747 Ganino, C., & Arndt, N. T. (2009). Climate changes caused by degassing of sediments during the
748 emplacement of large igneous provinces. *Geology*, 37(4), 323-326.
749
- 750 Garrels, R. M. (1965). Silica: role in the buffering of natural waters. *Science*, 148(3666), 69-69.
751

- 752 Gerlach, T. (2011). Volcanic versus anthropogenic carbon dioxide. *Eos, Transactions American*
753 *Geophysical Union*, 92(24), 201-202.
754
- 755 Gillis, K. M., & Coogan, L. A. (2011). Secular variation in carbon uptake into the ocean crust.
756 *Earth and Planetary Science Letters*, 302(3), 385-392.
757
- 758 Goldschmidt, V. M. (1912). Die Gesetze der Gesteinsmetamorphose mit Beispielen aus der
759 *Geologie des Südlichen Norwegens (The laws of rock metamorphism with examples*
760 *from the geology of southern Norway)*. *Vi denskapselskapets Skrifter*. 1.
761
- 762 Gorman, P. J., Kerrick, D. M., & Connolly, J. A. D. (2006). Modeling open system metamorphic
763 decarbonation of subducting slabs. *Geochemistry, Geophysics, Geosystems*, 7(4).
764
- 765 Harker, R. I., & Tuttle, O. F. (1956). Experimental data on the P_{CO_2} -T curve for the reaction;
766 calcite-quartz \leftrightarrow wollastonite + carbon dioxide. *American Journal of Science*, 254(4),
767 239-256.
768
- 769 Hilton, D. R., Fischer, T. P., & Marty, B. (2002). Noble gases and volatile recycling at
770 subduction zones. *Reviews in mineralogy and geochemistry*, 47(1), 319-370.
771
- 772 Högbom, A. (1894). Om sannolikheten för sekulära förändringar i atmosfärens kolsyrehalt (On
773 the probability of secular variations of atmospheric carbon dioxide). *Svensk kemisk*
774 *tidskrift*, 4, 169-177.
775
- 776 Holland, H. D. (1978). *The chemistry of the atmosphere and oceans*. Wiley: New York, NY.
777
- 778 Holland, T. J. B., & Powell, R. T. J. B. (1998). An internally consistent thermodynamic data set
779 for phases of petrological interest. *Journal of metamorphic Geology*, 16(3), 309-343.
780
- 781 Isson, T. T., & Planavsky, N. J. (2018). Reverse weathering as a long-term stabilizer of marine
782 pH and planetary climate. *Nature*, 560(7719), 471.
783
- 784 Jenny, H. (1941). *Factors of Soil Formation*. McGraw-Hill: New York, NY.
785
- 786 Kasting, J. F. (2010). Early Earth: faint young Sun redux. *Nature*, 464(7289), 687.
787
- 788 Kasting, J. F., Whitmire, D. P., & Reynolds, R. T. (1993). Habitable zones around main
789 sequence stars. *Icarus*, 101(1), 108-128.
790
- 791 Kelemen, P. B. & Matter, J. M. (2008) In situ carbonation of peridotite for CO₂ storage.
792 *Proceedings of the National Academy of Sciences, USA* 105, 17295–17300.
793
- 794 Kelemen, P. B., & Manning, C. E. (2015). Reevaluating carbon fluxes in subduction zones, what
795 goes down, mostly comes up. *Proceedings of the National Academy of Sciences*,
796 201507889.
797

- 798 Kelemen, P. B., Aines, R., Bennett, E., Benson, S. M., Carter, E., Coggon, J. A., ... & Godard,
799 M. (2018). In situ carbon mineralization in ultramafic rocks: Natural processes and
800 possible engineered methods. *Energy Procedia*, 146, 92-102.
801
- 802 Kennedy, W. Q. (1948). On the significance of thermal structure in the Scottish Highlands.
803 *Geological Magazine*, 85(4), 229-234.
804
- 805 Kerrick, D. M. (1977). The genesis of zoned skarns in the Sierra Nevada, California. *Journal of*
806 *petrology*, 18(1), 144-181.
807
- 808 Kerrick, D. M., & Caldeira, K. (1998). Metamorphic CO₂ degassing from orogenic belts.
809 *Chemical Geology*, 145(3-4), 213-232.
810
- 811 Kerrick, D. M., & Connolly, J. A. D. (2001). Metamorphic devolatilization of subducted marine
812 sediments and the transport of volatiles into the Earth's mantle. *Nature*, 411(6835), 293.
813
- 814 Knauth, L. P., & Epstein, S. (1976). Hydrogen and oxygen isotope ratios in nodular and bedded
815 cherts. *Geochimica et Cosmochimica Acta*, 40(9), 1095-1108.
816
- 817 Kump, L. R., & Arthur, M. A. (1999). Interpreting carbon-isotope excursions: carbonates and
818 organic matter. *Chemical Geology*, 161(1-3), 181-198.
819
- 820 Lagache, M. (1976). New data on the kinetics of the dissolution of alkali feldspars at 200 °C in
821 CO₂ charged water. *Geochimica et Cosmochimica Acta*, 40(2), 157-161.
822
- 823 Lal, R. (2008). Carbon sequestration. *Philosophical Transactions of the Royal Society of London*
824 *B: Biological Sciences*, 363(1492), 815-830.
825
- 826 Le Voyer, M., Hauri, E. H., Cottrell, E., Kelley, K. A., Salters, V. J., Langmuir, C. H., ... & Füre,
827 E. (2019). Carbon fluxes and primary magma CO₂ contents along the global mid-ocean
828 ridge system. *Geochemistry, Geophysics, Geosystems*, 20.
829
- 830 Lechat, K., Lemieux, J. M., Molson, J., Beaudoin, G., & Hébert, R. (2016). Field evidence of
831 CO₂ sequestration by mineral carbonation in ultramafic milling wastes, Thetford Mines,
832 Canada. *International Journal of Greenhouse Gas Control*, 47, 110-121.
833
- 834 Lee, C. T. A., Shen, B., Slotnick, B. S., Liao, K., Dickens, G. R., Yokoyama, Y., ... & Schneider,
835 T. (2013). Continental arc–island arc fluctuations, growth of crustal carbonates, and long-
836 term climate change. *Geosphere*, 9(1), 21-36.
837
- 838 Li, J., Redfern, S.T.A., & Giovannelli, D. (2019). Introduction: Deep carbon cycle through five
839 reactions. *American Mineralogist*, 104(4): 465-467.
840
- 841 Loughnan, F. C. (1969). Chemical weathering of the silicate minerals (No. 549.6 L6).
842
- 843 Lyubetskaya, T., & Ague, J. J. (2010). Modeling metamorphism in collisional orogens intruded

- 844 by magmas: I. Thermal evolution. *American Journal of Science*, 310(6), 427-458.
845
- 846 Mackenzie, F. T., & Garrels, R. M. (1966). Chemical mass balance between rivers and oceans.
847 *American Journal of Science*, 264(7), 507-525.
848
- 849 Maher, K., & Chamberlain, C. P. (2014). Hydrologic regulation of chemical weathering and the
850 geologic carbon cycle. *Science*, 343(6178), 1502-1504.
851
- 852 Manabe, S., & Stouffer, R. J. (1993). Century-scale effects of increased atmospheric CO₂ on the
853 ocean-atmosphere system. *Nature*, 364(6434), 215.
854
- 855 Marty, B., & Tolstikhin, I. N. (1998). CO₂ fluxes from mid-ocean ridges, arcs and plumes.
856 *Chemical Geology*, 145(3), 233-248.
857
- 858 Mason, E., Edmonds, M., & Turchyn, A. V. (2017). Remobilization of crustal carbon may
859 dominate volcanic arc emissions. *Science*, 357(6348), 290-294.
860
- 861 Matter, J. M., Stute, M., Snæbjörnsdóttir, S. Ó., Oelkers, E. H., Gislason, S. R., Aradóttir, E. S.,
862 ... & Axelsson, G. (2016). Rapid carbon mineralization for permanent disposal of
863 anthropogenic carbon dioxide emissions. *Science*, 352(6291), 1312-1314.
864
- 865 Meybeck, M. (1979). Concentrations des eaux fluviales en éléments majeurs et apports en
866 solution aux océans (Concentrations of major elements in fluvial waters and solutions in
867 the oceans), *Revue de Géologie Dynamique et de Géographie Physique.*, 21, 215-246.
868
- 869 Miyashiro, A. (1972). Metamorphism and related magmatism in plate tectonics. *American*
870 *Journal of Science*, 272(7), 629-656.
871
- 872 Mojzsis, S. J., Harrison, T. M., & Pidgeon, R. T. (2001). Oxygen-isotope evidence from ancient
873 zircons for liquid water at the Earth's surface 4,300 Myr ago. *Nature*, 409(6817), 178.
874
- 875 Nabelek, P. I., Bédard, J. H., & Rainbird, R. H. (2014). Numerical constraints on degassing of
876 metamorphic CO₂ during the Neoproterozoic Franklin large igneous event, Arctic
877 Canada. *Bulletin*, 126(5-6), 759-772.
878
- 879 O'Connor, W. K., Dahlin, D. C., Nilsen, D. N., Rush, G. E., Walters, R. P., & Turner, P. C.
880 (2001). Carbon dioxide sequestration by direct mineral carbonation: results from recent
881 studies and current status (No. DOE/ARC-2001-029). Albany Research Center (ARC),
882 Albany, OR.
883
- 884 Orme, D. A. (2015). Basin evolution and exhumation of the Xigaze forearc and Indus-Yarlung
885 suture zone, Tibet. PhD Thesis at The University of Arizona.
886
- 887 Owen, T., Cess, R. D., & Ramanathan, V. (1979). Enhanced CO₂ greenhouse to compensate for
888 reduced solar luminosity on early Earth. *Nature*, 277(5698), 640.
889

- 890 Pan D, Galli G (2016) The fate of carbon dioxide in water-rich fluids under extreme conditions.
891 Science Advances 2(10):e1601278-e1601278
892
- 893 Park, A. H. A., & Fan, L. S. (2004). CO₂ mineral sequestration: physically activated dissolution
894 of serpentine and pH swing process. Chemical Engineering Science, 59(22-23), 5241-
895 5247.
896
- 897 Penniston-Dorland, S. C., & Ferry, J. M. (2006). Development of spatial variations in reaction
898 progress during regional metamorphism of micaceous carbonate rocks, northern New
899 England. American Journal of Science, 306(7), 475-524.
900
- 901 Piccoli, F., Brovarone, A. V., Beyssac, O., Martinez, I., Ague, J. J., & Chaduteau, C. (2016).
902 Carbonation by fluid–rock interactions at high-pressure conditions: implications for
903 carbon cycling in subduction zones. Earth and Planetary Science Letters, 445, 146-159.
904
- 905 Piccoli, F., Brovarone, A. V., & Ague, J. J. (2018). Field and petrological study of metasomatism
906 and high-pressure carbonation from lawsonite eclogite-facies terrains, Alpine Corsica.
907 Lithos, 304, 16-37.
908
- 909 Plank, T., & Langmuir, C. H. (1998). The chemical composition of subducting sediment and its
910 consequences for the crust and mantle. Chemical geology, 145(3), 325-394.
911
- 912 Poli, S. (2015). Carbon mobilized at shallow depths in subduction zones by carbonatitic liquids.
913 Nature Geoscience, 8(8), 633.
914
- 915 Power, I. M., Harrison, A. L., & Dipple, G. M. (2016). Accelerating mineral carbonation using
916 carbonic anhydrase. Environmental science & technology, 50(5), 2610-2618.
917
- 918 Rahman, S., Aller, R. C., & Cochran, J. K. (2017). The missing silica sink: Revisiting the marine
919 sedimentary Si cycle using cosmogenic ³²Si. Global Biogeochemical Cycles, 31(10),
920 1559-1578.
921
- 922 Raymo, M. E., & Ruddiman, W. F. (1992). Tectonic forcing of late Cenozoic climate. Nature,
923 359(6391), 117.
924
- 925 Ronov, A. B., Yaroshevskii, A. A., & Migdisov, A. A. (1990). Chemical Structure of the Earth's
926 Crust and Geochemical Balance of Major Elements.
927
- 928 Royer, D. L., Berner, R. A., Montañez, I. P., Tabor, N. J., & Beerling, D. J. (2004). CO₂ as a
929 primary driver of phanerozoic climate. GSA today, 14(3), 4-10.
930
- 931 Rumble, D., Ferry, J. M., Hoering, T. C., & Boucot, A. J. (1982). Fluid flow during
932 metamorphism at the Beaver Brook fossil locality, New Hampshire. American Journal of
933 Science, 282(6), 886-919.
934
- 935 Sagan, C. (1962). Structure of the lower atmosphere of Venus. Icarus, 1(1-6), 151-169.

- 936
937 Sagan, C., & Mullen, G. (1972). Earth and Mars: Evolution of atmospheres and surface
938 temperatures. *Science*, 177(4043), 52-56.
939
940 Sakai, H., Gamo, T., Kim, E. S., Tsutsumi, M., Tanaka, T., Ishibashi, J., ... & Oomori, T. (1990).
941 Venting of carbon dioxide-rich fluid and hydrate formation in mid-Okinawa trough
942 backarc basin. *Science*, 248(4959), 1093-1096.
943
944 Sano, Y., & Williams, S. N. (1996). Fluxes of mantle and subducted carbon along convergent
945 plate boundaries. *Geophysical Research Letters*, 23(20), 2749-2752.
946
947 Scambelluri, M., Bebout, G. E., Belmonte, D., Gilio, M., Campomenosi, N., Collins, N., &
948 Crispini, L. (2016). Carbonation of subduction-zone serpentinite (high-pressure
949 ophicarbonate; Ligurian Western Alps) and implications for the deep carbon cycling.
950 *Earth and Planetary Science Letters*, 441, 155-166.
951
952 Sieber, M. J., Hermann, J., & Yaxley, G. M. (2018). An experimental investigation of C-O-H
953 fluid-driven carbonation of serpentinites under forearc conditions. *Earth and Planetary
954 Science Letters*, 496, 178-188.
955
956 Siever, R. (1968). Sedimentological consequences of a steady-state ocean-atmosphere.
957 *Sedimentology*, 11(1-2), 5-29.
958
959 Sillén, L. G. (1961). The physical chemistry of sea water. *Oceanography* 67, 549–581.
960
961 Sleep, N. H., & Zahnle, K. (2001). Carbon dioxide cycling and implications for climate on
962 ancient Earth. *Journal of Geophysical Research: Planets*, 106(E1), 1373-1399.
963
964 Solomon, E. A., Spivack, A. J., Kastner, M., Torres, M. E., & Robertson, G. (2014). Gas hydrate
965 distribution and carbon sequestration through coupled microbial methanogenesis and
966 silicate weathering in the Krishna–Godavari basin, offshore India. *Marine and Petroleum
967 Geology*, 58, 233-253.
968
969 Staudigel, H., Hart, S. R., Schmincke, H. U., & Smith, B. M. (1989). Cretaceous ocean crust at
970 DSDP Sites 417 and 418: Carbon uptake from weathering versus loss by magmatic
971 outgassing. *Geochimica et Cosmochimica Acta*, 53(11), 3091-3094.
972
973 Stewart, E. M., & Ague, J. J. (2018). Infiltration-driven metamorphism, New England, USA:
974 Regional CO₂ fluxes and implications for Devonian climate and extinctions. *Earth and
975 Planetary Science Letters*, 489, 123-134.
976
977 Sverjensky, D. A., Stagno, V., & Huang, F. (2014). Important role for organic carbon in
978 subduction-zone fluids in the deep carbon cycle. *Nature Geoscience*, 7(12), 909.
979
980 Tao, R., Zhang, L., Li, S., Zhu, J., & Ke, S. (2018). Significant contrast in the Mg-C-O isotopes

- 981 of carbonate between carbonated eclogite and marble from the SW Tianshan UHP
982 subduction zone: Evidence for two sources of recycled carbon. *Chemical Geology*, 483,
983 65-77.
984
- 985 Tian, M., & Ague, J. J. (2014). The impact of porosity waves on crustal reaction progress and
986 CO₂ mass transfer. *Earth and Planetary Science Letters*, 390, 80-92.
987
- 988 Tracy, R. J., Rye, D. M., Hewitt, D. A., & Schiffries, C. M. (1983). Petrologic and stable-
989 isotopic studies of fluid-rock interactions, south-central Connecticut: I. The role of
990 infiltration in producing reaction assemblages in impure marbles. *American Journal of*
991 *Science*, 283, 589-616.
992
- 993 Urey, H.C. (1952). *The Planets: Their Origin and Development*. New Haven, CT: Yale
994 University Press.
995
- 996 Varekamp, J. C., Kreulen, R., Poorter, R. P. E., & Van Bergen, M. J. (1992). Carbon sources in
997 arc volcanism, with implications for the carbon cycle. *Terra Nova*, 4(3), 363-373.
998
- 999 Walker, J. C., Hays, P. B., & Kasting, J. F. (1981). A negative feedback mechanism for the long-
1000 term stabilization of Earth's surface temperature. *Journal of Geophysical Research:*
1001 *Oceans*, 86(C10), 9776-9782.
1002
- 1003 Wallmann, K., Aloisi, G., Haeckel, M., Tishchenko, P., Pavlova, G., Greinert, J., ... &
1004 Eisenhauer, A. (2008). Silicate weathering in anoxic marine sediments. *Geochimica et*
1005 *Cosmochimica Acta*, 72(12), 2895-2918.
1006
- 1007 White, A. F., & Blum, A. E. (1995). Effects of climate on chemical weathering in watersheds.
1008 *Geochimica et Cosmochimica Acta*, 59(9), 1729-1747.
1009
- 1010 Wilde, S. A., Valley, J. W., Peck, W. H., & Graham, C. M. (2001). Evidence from detrital
1011 zircons for the existence of continental crust and oceans on the Earth 4.4 Gyr ago. *Nature*,
1012 409(6817), 175.
1013
- 1014 Wilson, S. A., Dipple, G. M., Power, I. M., Thom, J. M., Anderson, R. G., Raudsepp, M., ... &
1015 Southam, G. (2009). Carbon dioxide fixation within mine wastes of ultramafic-hosted ore
1016 deposits: Examples from the Clinton Creek and Cassiar chrysotile deposits, Canada.
1017 *Economic Geology*, 104(1), 95-112.
1018
- 1019 Winnick, M. J., & Maher, K. (2018). Relationships between CO₂, thermodynamic limits on
1020 silicate weathering, and the strength of the silicate weathering feedback. *Earth and*
1021 *Planetary Science Letters*, 485, 111-120.
1022
- 1023

1024

Figure Captions

1025 **Figure 1.** Schematic cross section showing the tectonic context of major carbonation /
1026 decarbonation processes. Sources of atmospheric CO₂ are indicated in red whereas sinks are in
1027 blue.

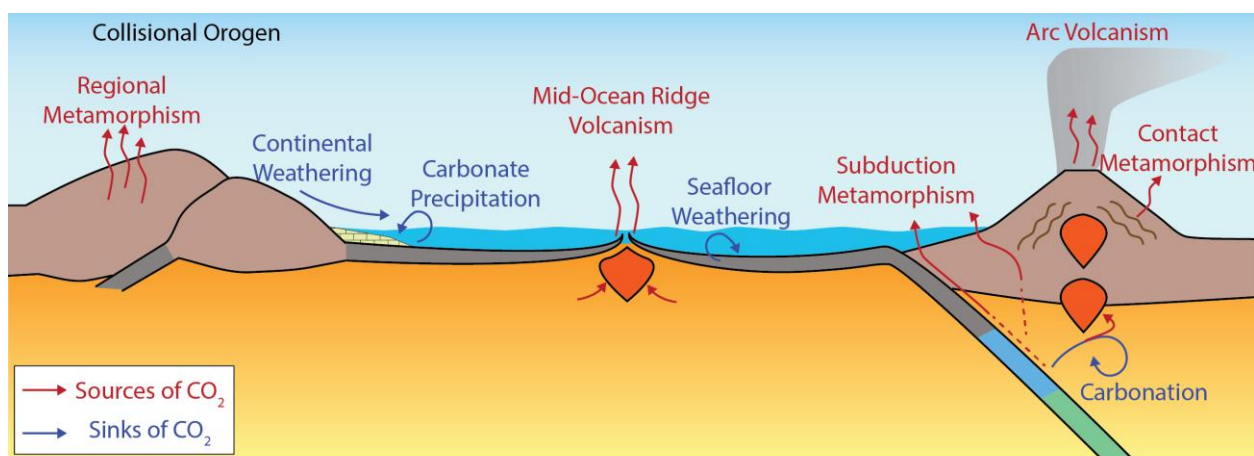
1028 **Figure 2.** Photographs of carbonation / decarbonation processes. (A) Silicate weathering: granite
1029 exposed at Earth's surface undergoes spheroidal weathering resulting in discrete boulders with
1030 thick physical and chemical weathering rinds. Volax, Tinos Island, Greece. (B) High temperature
1031 carbonation: yellow Ni-bearing calcite has precipitated in an ultramafic rock of the Maltby Lakes
1032 Metavolcanics, Connecticut. (C) Infiltration-driven decarbonation: quartz vein (center; Qz) with
1033 diopside (Di) + amphibole (Amp) + zoisite (Zo) selvages cutting biotite-bearing metacarbonate
1034 rock (dark margins; Bi) of the Wepawaug Schist, Connecticut. Prograde reactions, such as
1035 $\text{Phlogopite} + 3 \text{ Calcite} + 6 \text{ Quartz} = 3 \text{ Diopside} + \text{K-feldspar} + 3 \text{ CO}_2 + \text{H}_2\text{O}$, generated
1036 significant CO₂ (Ague 2003; Stewart and Ague 2018).

1037 **Figure 3.** Global map indicating the locations of modern subduction (red lines with carets), and
1038 ancient sutures formed in the Phanerozoic (blue) and Proterozoic (green). Sutures which were
1039 active during both eons are dashed blue and green. Modified after Orme (2015) and Burke *et al.*
1040 (1977).

1041 **Figure 4.** Pressure-Temperature diagram showing the stability of the assemblage calcite +
1042 quartz relative to wollastonite + CO₂. Conditions of this reaction are calculated for equilibrium
1043 between minerals and a fluid of differing CO₂ content (X_{CO_2} is the mole fraction of CO₂ in fluid).
1044 Calculations made using the program Theriak-Domino (de Capitani & Petrakakis 2010) with the
1045 Holland & Powell (1998) database.

1046 **Figure 5.** Estimates of modern CO₂ fluxes to the ocean–atmosphere system. Error bars indicate
1047 a range of possible values, not necessarily a normal distribution. *Note that the flux from Arc
1048 Volcanism includes some contribution from decarbonation of subducting slabs; in fact, slab
1049 decarbonation could account for the vast majority of the arc volcanic flux. Arc magmas may also
1050 incorporate partially melted carbonate lithologies and drive contact metamorphism in adjacent
1051 rocks.

1052 **Figure 6.** Predicted atmospheric CO₂ concentrations in an Earth system where CO₂ sources and
1053 sinks do not balance, modified after Berner & Caldeira (1997). Regardless of starting CO₂
1054 concentration, a 25% excess in CO₂ degassing (red curves) or a 25% excess in silicate
1055 weathering (blue curves) result in a run-away atmospheric composition within ~1 million years.



1056 **Figure 1**

1057

1058

1059

1060

1061

1062

1063

1064

1065

1066

1067



1068 **Figure 2**

1069

1070

1071

1072

1073

1074

1075

1076

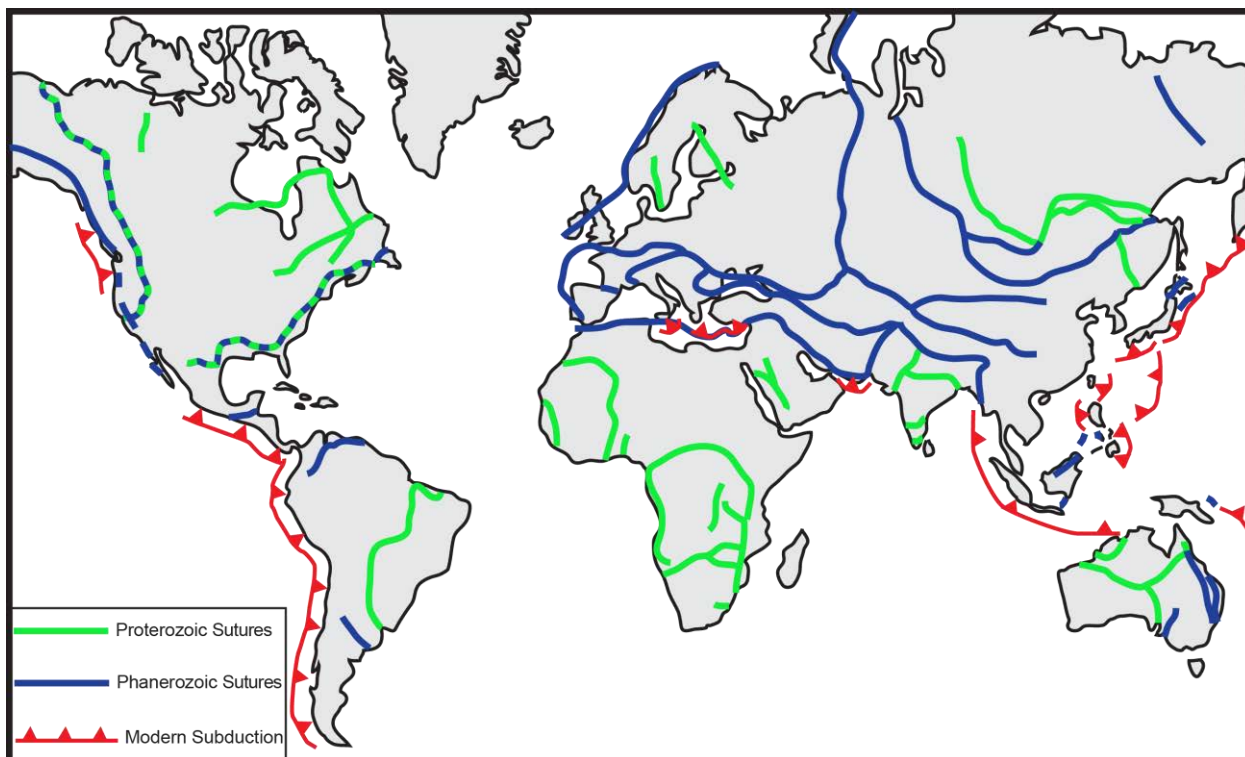
1077

1078

1079

1080

1081



1082

Figure 3

1083

1084

1085

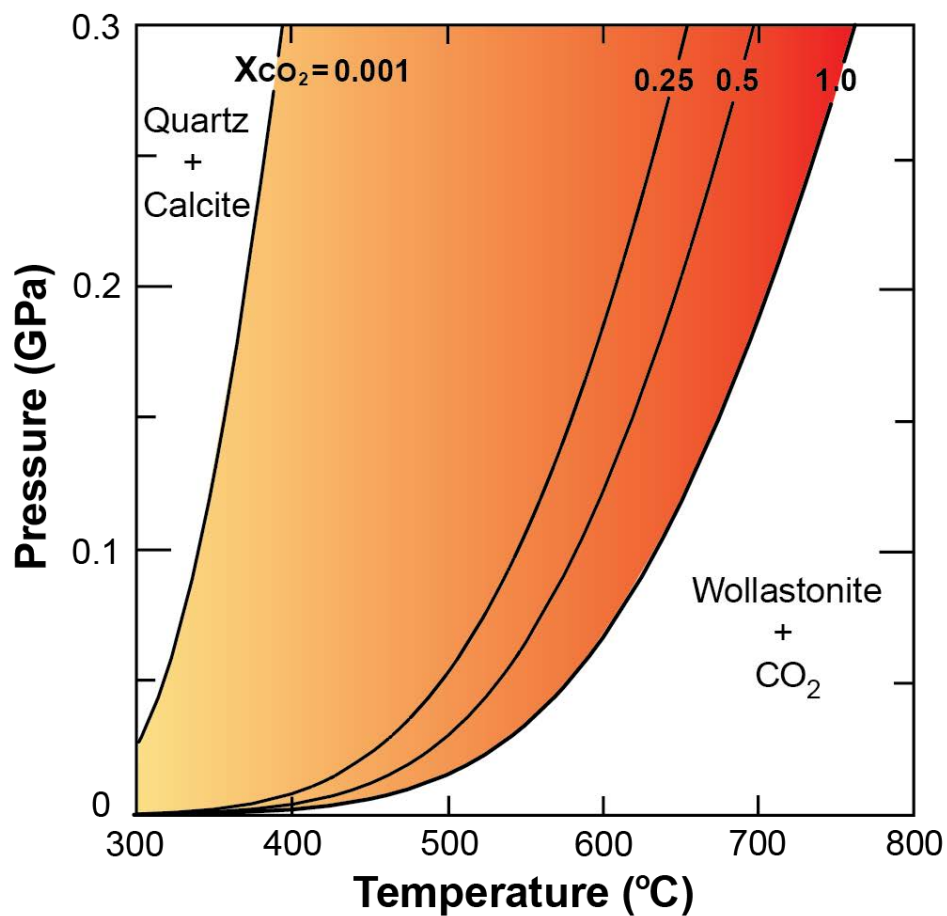


Figure 4

1086

1087

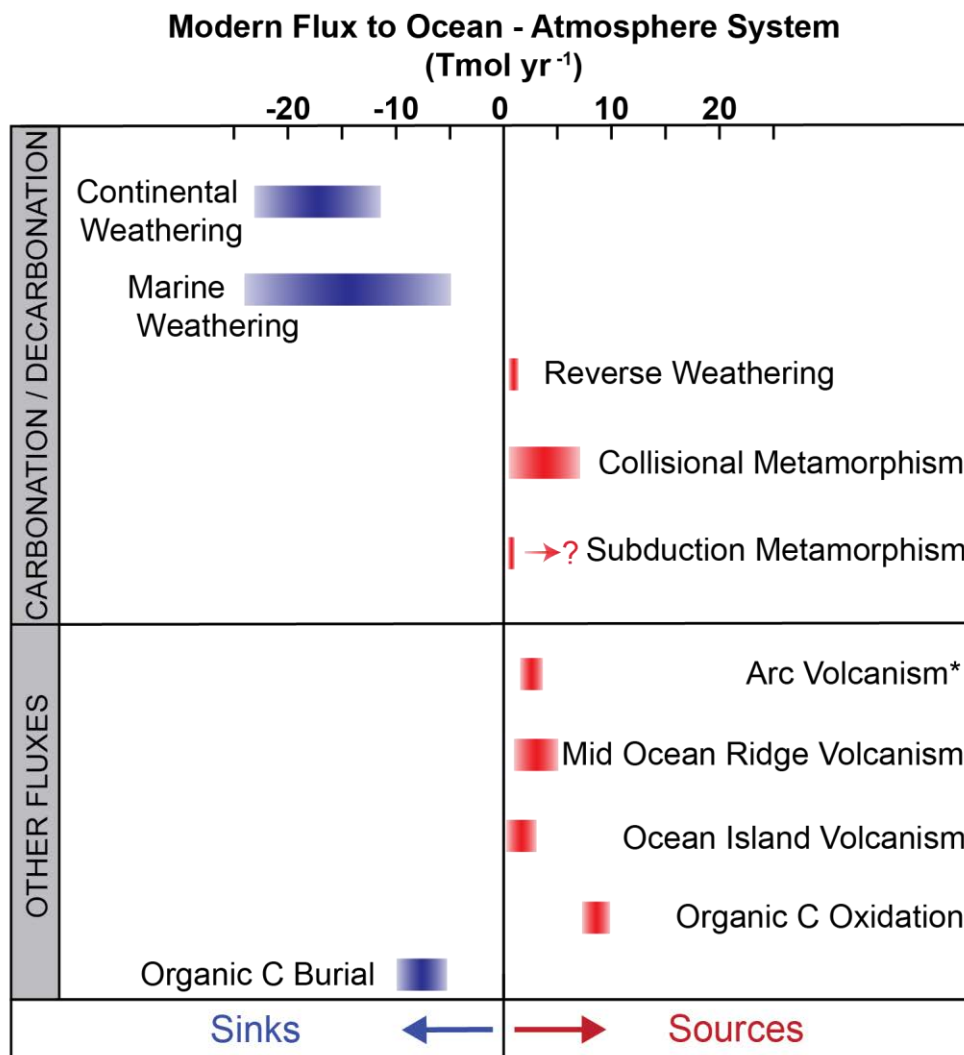
1088

1089

1090

1091

1092



1093

Figure 5

1094

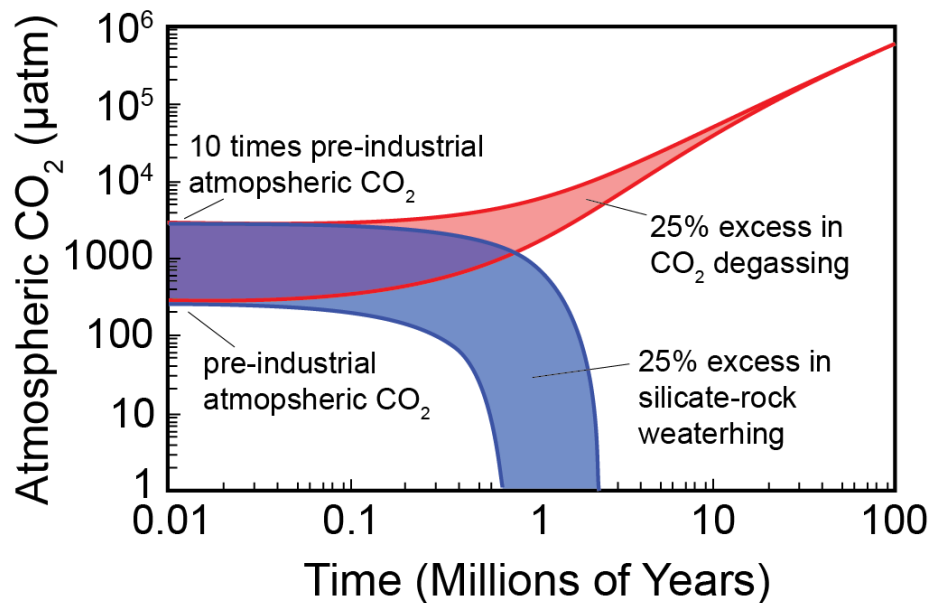
1095

1096

1097

1098

1099



1100

Figure 6

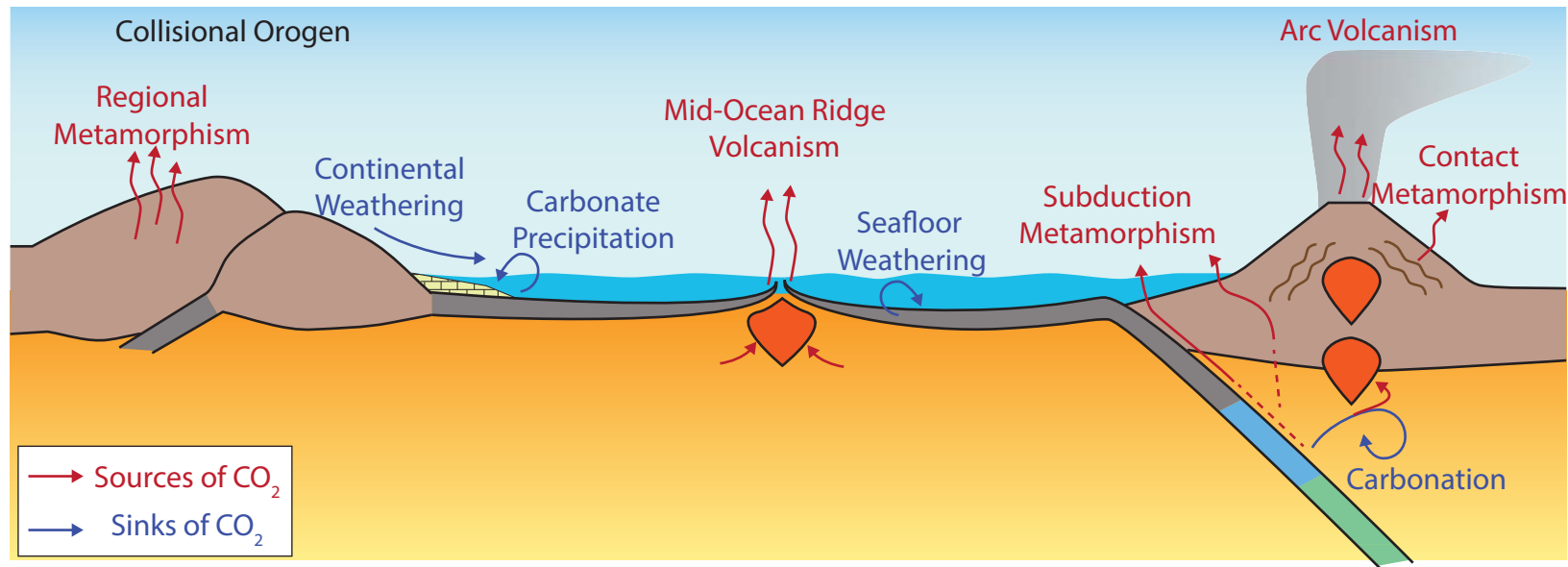


Figure 1



Figure 2

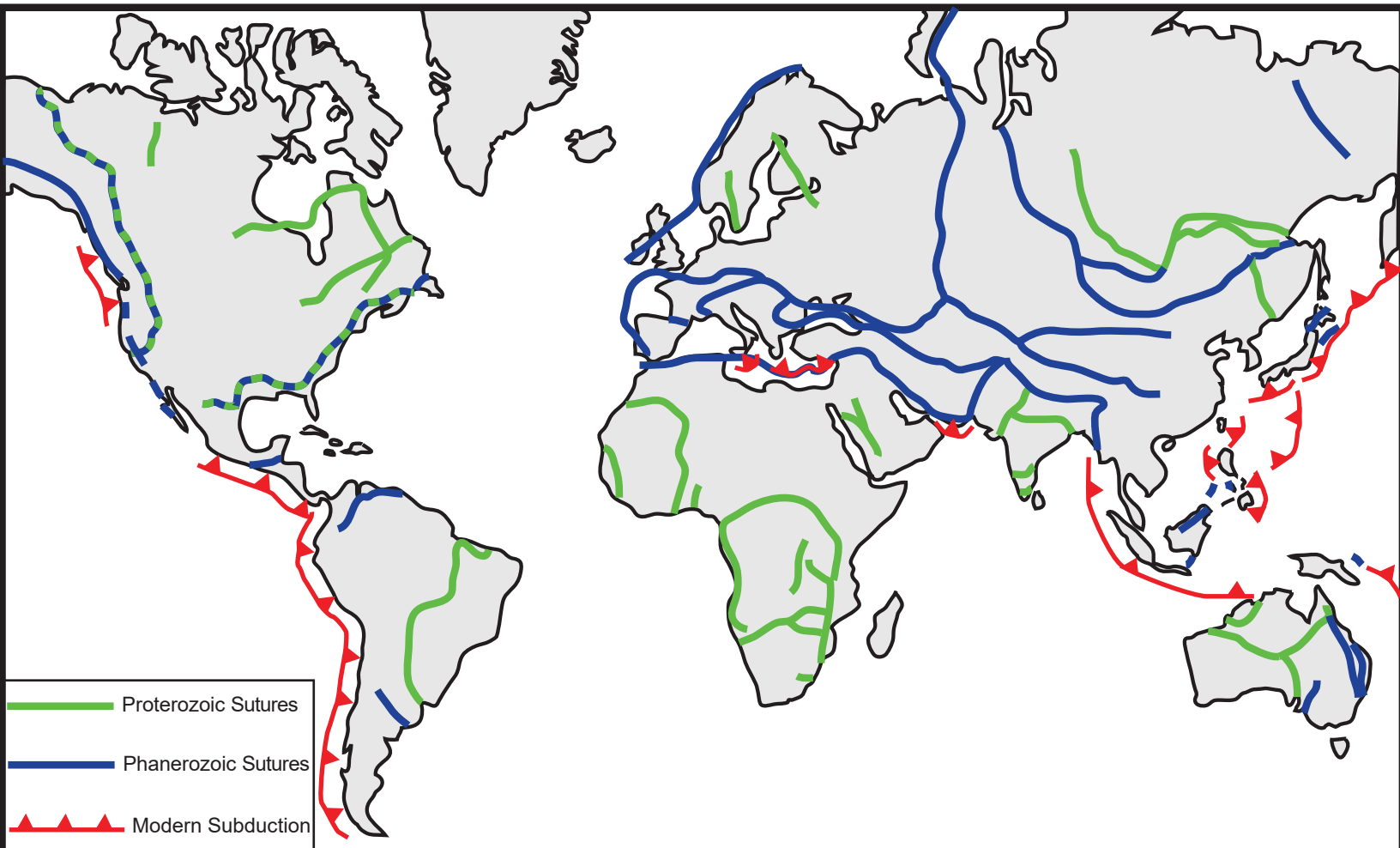


Figure 3

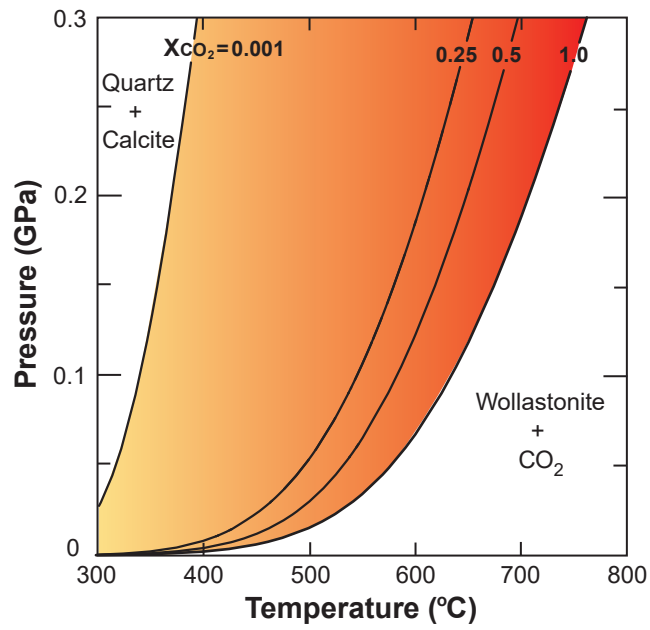


Figure 4

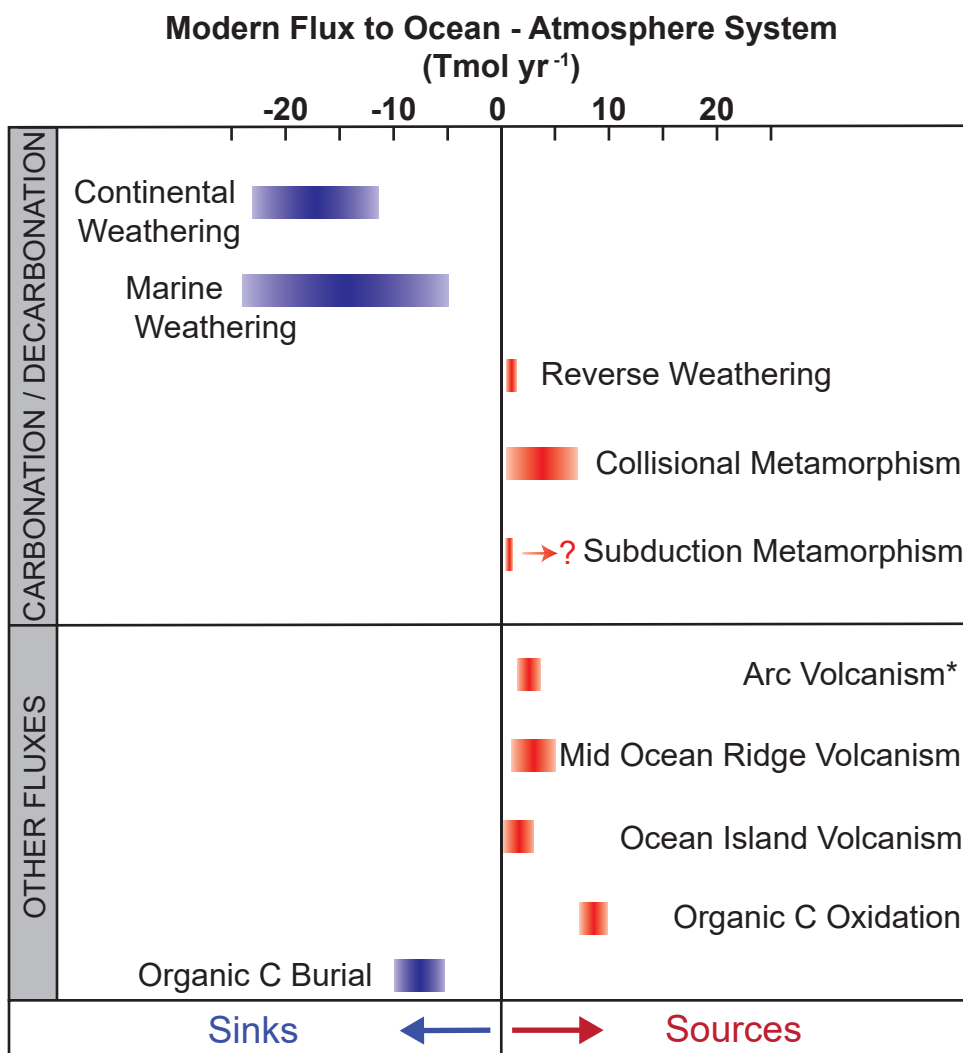


Figure 5

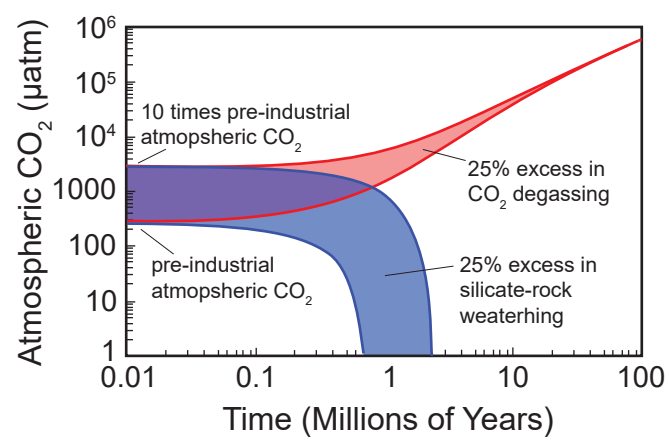


Figure 6